

# We are IntechOpen, the world's leading publisher of Open Access books Built by scientists, for scientists

6,900

Open access books available

185,000

International authors and editors

200M

Downloads

Our authors are among the

154

Countries delivered to

TOP 1%

most cited scientists

12.2%

Contributors from top 500 universities



WEB OF SCIENCE™

Selection of our books indexed in the Book Citation Index  
in Web of Science™ Core Collection (BKCI)

Interested in publishing with us?  
Contact [book.department@intechopen.com](mailto:book.department@intechopen.com)

Numbers displayed above are based on latest data collected.  
For more information visit [www.intechopen.com](http://www.intechopen.com)



---

# Plasmonics Devoted to Photocatalytic Applications in Liquid, Gas, and Biological Environments

---

Carlos J. Bueno-Alejo, Adriana Arca-Ramos and  
Jose L. Hueso

Additional information is available at the end of the chapter

<http://dx.doi.org/10.5772/intechopen.68812>

---

## Abstract

Plasmonic nanomaterials have emerged in the last years as a very interesting option for many photocatalytic processes. Their localized surface plasmon resonance (LSPR) brings in some unique properties that overcome some of the drawbacks associated with traditional photocatalysis based on semiconductors. Even when in its infancy, many advances have been made in the field, mainly related to the synthesis of new structures with the capabilities of light absorption in the whole solar spectrum. A great number of reactions have been attempted using nanoplasmonic materials. In this chapter, we present the most recent advances made in the field of plasmonic photocatalysis comprising an introductory section to define the main types of plasmonic nanomaterials available, including the most recently labeled alternatives. Following with the major areas of catalytic application, a second section of the chapter has been devoted to liquid-phase reactions for the treatment of pollutants and a selection of organic reactions to render added-value to chemicals under mild conditions. The third part of the chapter addresses two specific applications of nanoplasmonic photocatalysts in gas-phase reactions involving the remediation of volatile organic compounds and the transformation of carbon dioxide into valuable energy-related chemicals. Finally, a fourth section of the chapter introduces the most recent applications of plasmonics in biochemical processes involving the regulation of cofactor molecules and their mimetic behavior as potential enzyme-like surrogates.

**Keywords:** surface plasmon, photocatalysis, NIR, pollutants, energy, VOCs, CO<sub>2</sub>, semiconductor, mimetic enzymes

---

## 1. Introduction

Solar energy harvesting has become an important matter nowadays. The use of solar light as energy source is a cleaner and even a more economic way to provide energy to processes. In this sense, conventional photocatalysis, as it makes use of mainly semiconductors as catalyst, is not the most efficient way to harvest the light coming from the sun, since it only contains 5% of UV light, which is the kind of radiation necessary to excite those catalysts [1]. In the quest of new materials that could help to improve the efficiency of traditional photocatalyst, plasmonic nanomaterials have attracted much attention lately among the scientific community. This is so because this new family of materials offers/exhibits several advantages over their bulk counterparts that can be useful in very different fields like sensors, biomedicine, photocatalysis, etc [2]. Besides their size, what makes these materials so interesting is their characteristic localized surface plasmon resonance band (LSPR). This LSPR can be defined as the collective coherent oscillation of free charges on the surface of the nanoparticle when they are in resonance with the incident light. This resonance generates an enhancement in the electric field on the surface of the nanomaterials that may affect molecules or materials surrounding it. The LSPR can be very useful for photocatalysis in many different aspects depending mostly on the type of plasmonic material used. We have tentatively classified them into three main categories: (1) Pure plasmonic materials; (2) Hybrid plasmonic materials and (3) Alternative plasmonic materials.

### 1.1. Pure plasmonic materials

The photocatalysts belonging to this group are only composed by unsupported plasmonic metals and those supported on photocatalytic insulators allowing all the chemistry to happen on the metal nanomaterial. In this case, after excitation of the plasmon band, a high density of charge carriers are generated on the surface of the nanoparticle that can undergo reduction or oxidation reactions with the molecules adsorbed on their surfaces [3].

This mechanism is generally referred to as direct charge transfer since the carrier is directly transferred from higher energy levels in the metal to the lower unoccupied molecular orbital of the adsorbate initiating the chemical reaction (**Figure 1**). Another property of the plasmonic nanoparticles is the generation of heat on their vicinity. Following the excitation, the charges generated can suffer radiative or nonradiative relaxation. The former will be discussed later in this section. The nonradiative relaxation is mainly related with electron-electron and electron-phonon interactions, which give rise to the generation of heat, very localized in the surface of the nanoparticle. This heat can be transferred to the surrounding media, helping in thermally activated reactions. The temperature reached on the surface of the metal is dependent on the nature of the metal itself. For gold, it has been estimated to be as high as 500–700°C [4] and for silver, is expected to be much higher since the absorption cross section of the latter is around 10 times higher than for gold. An example of photocatalytic reaction performed by gold plasmonic nanoparticle (AuNP) is given by Hallet-Tapley et al., using them for the selective oxidation of alcohols [5]. They used green laser and LED in order to excite the plasmon

band of the AuNP and oxidize selectively the alcohol molecules surrounding the AuNP. In their work, the authors proposed two possible mechanisms for the reaction, one involving a single electron transfer from gold to  $\text{H}_2\text{O}_2$  providing the radicals that initiate a chain reaction, and the other implicating the generation of heat as the cause for the breaking of the peroxide bond. Another interesting example is the use of nanorattles composed of a gold nanosphere inside and a nanoshell of gold/silver [6]. In this case, the authors claim that the better performance of this structure comes from the formation of electromagnetic hot spots in the interface of the two different materials. These hot spots create a higher density of reactive oxygen species responsible for the oxidation reaction. In order to expand the absorption of light to the visible and even the IR part of the spectrum, many researchers have tried to synthesize anisotropic nanoparticles. One of these examples is the synthesis of hexagonal Pd nanoplates for their use in the Suzuki coupling reaction. Trinh et al. [7] were able to obtain plasmonic Pd nanoparticles with their plasmon band located along the visible and the near IR according to their aspect ratio. They used this LSPR to generate hot electrons with the energy to perform the Suzuki reaction on the surface of the catalyst.

In this group, we can also include nanomaterials consisting of metal nanoparticles supported on photochemical insulators. The latter means that since the bandgap of the material is too high, it cannot be excited in the visible or near UV part of the spectrum. Metal oxides like  $\text{ZrO}_2$ ,  $\text{Al}_2\text{O}_3$ , or  $\text{SiO}_2$  with bandgap energies above 5–6 eV are representative of this group. Liu et al. [8] performed a selective reduction of nitrocompounds to the azoxy derivatives using Ag-Cu alloy nanoparticles supported on  $\text{ZrO}_2$ . They demonstrated that by irradiating in the

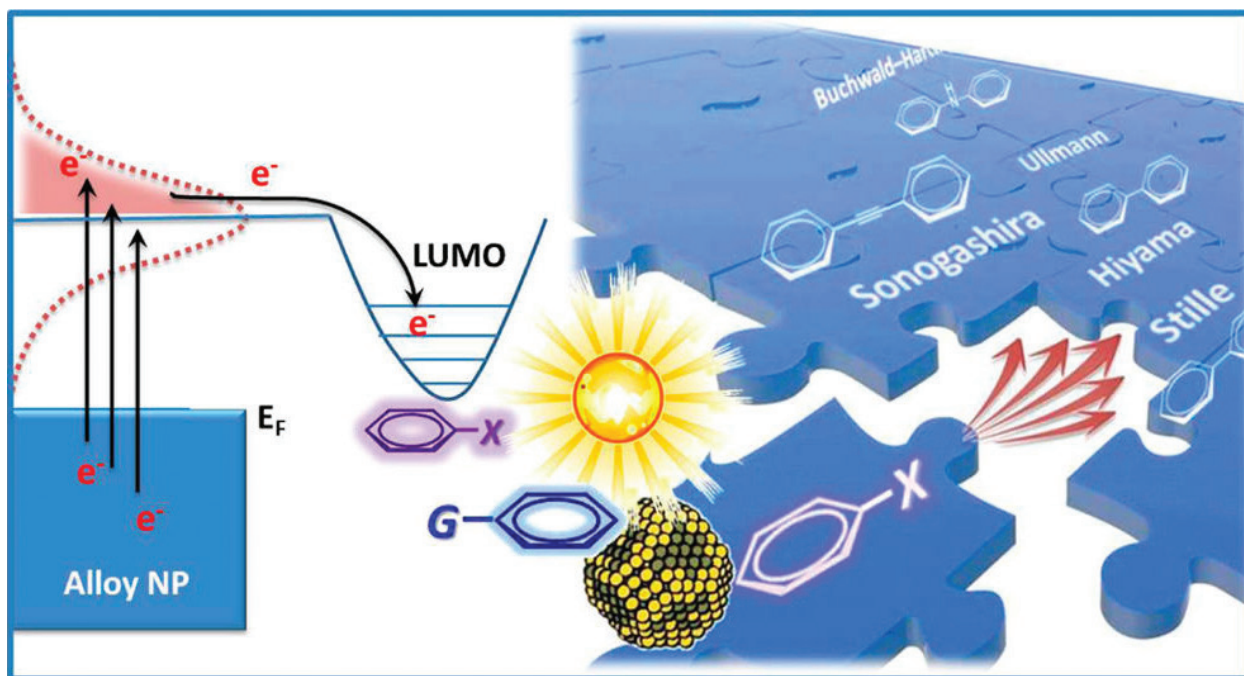


**Figure 1.** Typical mechanism of pure plasmonic materials. Reprinted with permission from Ref. [3]. Copyright (2014) American Chemical Society.

visible region, they could control the selectivity of the reaction only with the composition of alloy with no influence from the support.

## 1.2. Hybrid plasmonic materials

Semiconductors photocatalysts have dominated the field since Fujishima and Honda used  $\text{TiO}_2$  to do water splitting with UV light in 1972 [9]. Despite the convenient properties of this semiconductor for photocatalysis, it also has some drawbacks in order to use them in real photocatalytic applications like low photon efficiency, high charge carriers recombination rate and a high bandgap (3.2 eV), that means it can only be excited with UV light. To overcome these problems, great efforts have been devoted in the past years to develop a new family of photocatalysts consisting of supporting metal plasmonic nanoparticles on the surface of semiconductors. The metal nanoparticle brings in some properties that complement and fix some of the downsides previously mentioned for the semiconductors (**Figure 2**). First, they enhance the absorption of light by the material. They do this in different ways. The plasmon bands of the metal nanoparticles are usually in the visible region, expanding the absorption of the hybrid material to the visible or even near IR. Also, the huge absorption extinction coefficient of plasmonic materials allows them to absorb most of the light incoming to the hybrid, therefore, keeping most of the photon absorbed on the surface of the material, avoiding in a high extent the recombination of carriers that usually takes place in the semiconductor. Another feature of these materials that aids the absorption of light is the scattering. Plasmonic nanoparticles can scatter part of the light that are not able to absorb, thereby allowing its reemission and potential absorption by other nanoparticles allocated on its vicinity and increasing the pathway of light absorbed by the material. Another characteristic of these materials is the formation of what is called Schottky barrier between the metal and the semiconductor. In that interface, an electric field is built in that separates the charge carriers formed in or close to the barrier, avoiding in that way of the recombination of electron and holes, and therefore increasing the lifetime of those carriers, so they can react with other molecules adsorbed on the surface.

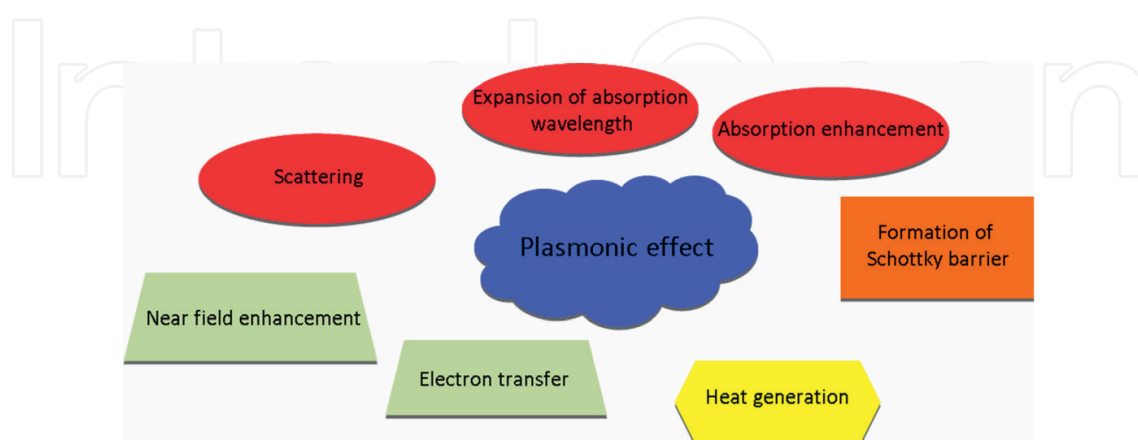


**Figure 2.** Different plasmonic effects in hybrid plasmonic structures. Different colors and shapes are used to identify each of them: absorption (red oval), structural (orange square), nonradiative (yellow hexagon) and radiative (green trapezium).



Besides absorption, plasmonic materials contribute to improve the photocatalytic performance of semiconductors through other mechanisms. After absorption of light, the excited electrons reach high-energy levels, so they can overcome the Schottky barrier formed between the metal and the semiconductor, and can be transferred from the nanoparticle to the semiconductor and start the photocatalytic process. This electron transfer means that a material that was only viable before for use with UV light due to its high bandgap, now can be used in almost any wavelength, because the shape and size of these metal nanoparticles can be tailored to have the plasmon band in the visible or even in the IR region of the spectrum. This is a very important feature when we think about the use of these materials under solar light illumination, since the excitation area can be expanded to the other 95% of the solar spectrum. Other mechanism by which plasmonic materials can enhance the photocatalytic performance of semiconductors is by the generation of an intensive local electric field that can promote/enhance the generation of more charge carriers on the surface of the semiconductors. Because of this electric field, plasmonic nanoparticles can also generate charge carriers without any contact with the support, which is beneficial when the contact between the metal and the semiconductor is not well enough to form a Schottky barrier, or when a layer of other material is needed to support the nanoparticles. It has also been probed that this electric field may help to polarize nonpolar molecules surrounding the metal nanoparticles and increase their adsorption to the surface of the semiconductor. Finally, another important feature of the plasmonic materials that enhances the photocatalytic response of these hybrid systems is the generation of heat on the vicinity of the nanoparticles. The high temperature generated in highly localized points can improve the reactions rate and the mass transfer in the reaction system.

Due to these properties, plasmonic hybrid materials are certainly a very interesting option to make some industrial processes environmentally and economically attractive.

### 1.3. Alternative plasmonic materials

Until very recently, nonmetal materials considered were not able to hold a LSPR due to the low free charge carrier concentration on their surface. However, lately many studies have probed that a whole variety of materials can be tuned to increase the free carrier concentration, and therefore be able to behave as plasmonic materials in the visible and IR regions [10]. Usually, doping the structure of metal oxides or adding oxygen vacancies increase the concentration of free electron within the metal oxide, and is a good way to get a plasmonic material. Examples of this are oxides of aluminum, zinc, cadmium, or tungsten, which after doping with different element acquire plasmonic characteristics in the visible or IR region due to the increase of the electron concentration [11]. Creating oxygen vacancies is also possible to get an analogous effect. For instance, tungsten oxide renders a plasmonic behavior in the IR, allowing their use in photocatalytic applications after the induced generation of oxygen vacancies [12]. A different circumstance happens with chalcogenides like CuS, in which the reduction of the Cu percentage creates an increase of the hole concentration, which results in a wide plasmon band in the IR region (**Figure 3**) [13]. All these materials are suitable to act as plasmonic photocatalysts with any of the mechanisms mentioned before.

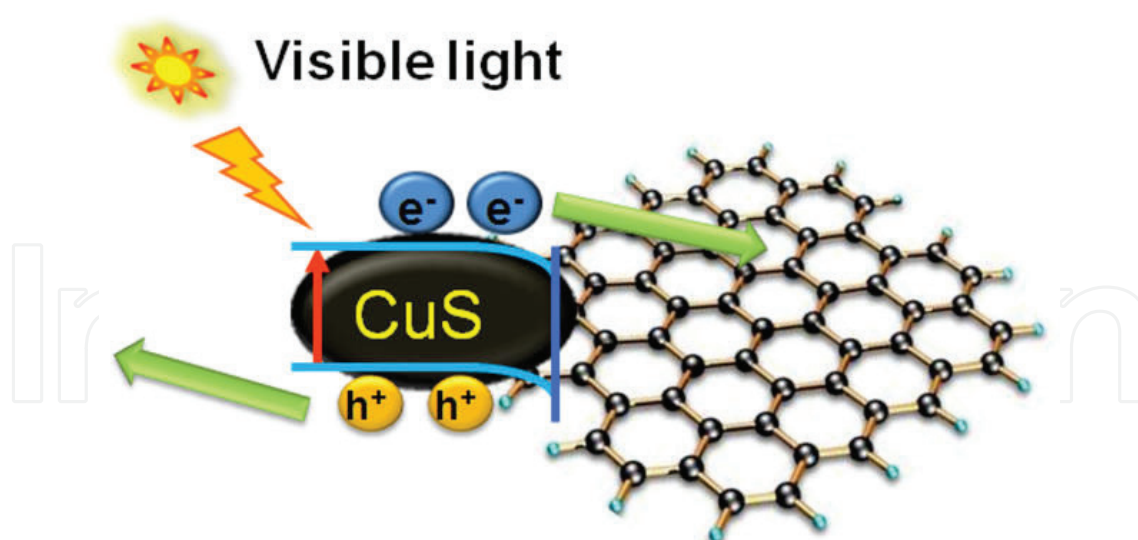


**Figure 3.** Schematic diagram (not to scale) to illustrate the energy level alignment and photocharge carrier dissociation at the CuS-RGO interface. Reprinted with permission from Ref. [13]. Copyright (2012) American Chemical Society.

## 2. Nanoplasmonic photocatalysis in liquid phase

### 2.1. Plasmonic-driven photocatalytic degradation of aqueous contaminants

Heterogeneous photocatalysis has been demonstrated as an economical and effective technology to remove organic pollutants from aqueous environments [14, 15]. In recent years, the LSPR effect of plasmonic materials has been applied to boost the photocatalytic performance of chemical transformations under visible light irradiation. A vast number of studies have focused on the preparation of plasmonic nanostructures and further application for the removal of pollutants from aqueous media. As there are some previous reviews reporting the use of plasmonic materials for pollutant removal [16–18], in this section we only show some recent applications on this topic, aiming at illustrating various types of plasmonic photocatalysts as well as target contaminants. These are summarized in **Table 1**.

Among the target pollutants, dyes such as rhodamine B (RhB), methylene blue (MB), or methyl orange (MO) are the most studied ones due to the ease of monitoring their removal. Nevertheless, in dye compounds the effect of photosensitization could produce extra electrons and accelerate the photocatalytic process. For this reason, the photoremediation of colorless target contaminants represents a more interesting case study [19]. For instance, the photocatalytic removal of other organic pollutants such as phenolic compounds, including bisphenol A, nitrophenol, and chlorophenols, antibiotics such as tetracycline or ciprofloxacin, organic solvent as trichloroethylene or even chlorinated paraffins have also been reported and summarized in **Table 1**. In addition to organic pollutants, this technology has been successfully applied for the treatment of hazardous inorganic compounds, such as the reduction of carcinogenic Cr (VI), from  $K_2Cr_2O_7$  to Cr (III) [20].

Catalyst	Pollutant	Irradiation	Performance	Refs.
Ag@g-C <sub>3</sub> N <sub>4</sub> @BiVO <sub>4</sub>	TC	300 W Xe lamp, $\lambda > 350$ nm, $\lambda > 420$ nm or $\lambda > 760$ nm	Removal of 90.8% ( $\lambda > 350$ nm), 82.7% ( $\lambda > 420$ nm), and 12.6 % ( $\lambda > 760$ nm) in 60 min	[27]
Ag <sub>2</sub> SO <sub>3</sub> /AgBr GO/Ag <sub>2</sub> SO <sub>3</sub> /AgBr	MO, RhB, MB	500 W Xe lamp, $\lambda > 420$ nm, 100 mW/cm <sup>2</sup>	99.9% removal of MO in 9 min, almost complete removal of RhB and MB in 20 min	[28]
Ag/AgCl-Bi <sub>2</sub> WO <sub>6</sub> @Fe <sub>3</sub> O <sub>4</sub> @SiO <sub>2</sub>	RhB, Phenol	300 W halogen tungsten projector lamp, $\lambda > 410$ nm	100% RhB removal in 90 min ~70% Phenol removal in 300 min	[19]
Pd/PdCl <sub>2</sub> -Bi <sub>2</sub> MoO <sub>6</sub>	Phenol	300 W halogen tungsten projector lamp, $\lambda > 410$ nm	22.2% removal in 30 min and almost 100% removal in 300 min	[26]
g-C <sub>3</sub> N <sub>4</sub> @Bi@Bi <sub>2</sub> WO <sub>6</sub>	2,4-DCP, MO, RhB	300 W Xe lamp, $\lambda > 400$ nm	~70% removal of MO and 2,4-DCP, and almost complete removal of RhB in 120 min	[22]
Ag@AgCl/TP	RhB, X-3B, CIP, phenol	300 W Xe lamp, $\lambda > 400$ nm	Complete removal of RhB in 8 min and of X-3B in 12 min, 48% CIP removal and 51% phenol removal in 3 h	[29]
Au-Fe-doped Bi <sub>4</sub> Ti <sub>3</sub> O <sub>12</sub> (BTO) nanosheets	Phenol, BPA	400 W halogen lamp, VIS light	BPA removal of 72%, 87%, 99% on pure BTO, 2%Fe/BTO and Au-2%Fe/BTO, respectively, in 50 min Phenol removal of 37, 54, and 64% on BTO, 2% Fe/BTO, and Au-2% Fe/BTO, respectively, in 80 min	[30]
Bi/Bi <sub>2</sub> WO <sub>6</sub>	RhB, 4-CP	300 W Xe lamp, $\lambda > 400$ nm, 200 mW/cm <sup>2</sup>	93.0% removal of RhB in 25 min, 54.4% removal of 4-CP in 120 min	[23]
TiO <sub>2</sub> /SiO <sub>2</sub> /Au (bipyramid-like gold nanoparticles)	FA	LED lamp (400–800 nm), 156 mW/cm <sup>2</sup> for tests in VIS region, high-pressure Hg lamp for tests in UVA + VIS region	With UVA + VIS irradiation, 58% removal in 1 h No photocatalytic activity under VIS irradiation alone	[31]
Au/BiOCl@mesoporous SiO <sub>2</sub>	FAD, RhB	350 W Xe lamp, $\lambda > 420$ nm	For FAD removal, the CO <sub>2</sub> evolution is ca. 49-fold higher than that of N-TiO <sub>2</sub> NPs (used as standard VIS light photocatalyst) ~100% removal of RhB in 1 h	[32]
RGO/CoFe <sub>2</sub> O <sub>4</sub> /Ag	Short chain chlorinated paraffins	500 W Xe lamp, $\lambda > 400$ nm, 60 mW/cm <sup>2</sup>	91.9% removal in 12 h	[33]
Ag/Ag <sub>2</sub> CO <sub>3</sub> -RGO	MO Phenol	350 W Xe lamp, $\lambda > 420$ nm 40 mW/cm <sup>2</sup>	93% MO removal in 15 min, 93% phenol removal in 30 min	[34]
Pt-BiOBr heterostructures	PNP, TBBPA	300 W Xe lamp Simulated sunlight (320–680 nm) or VIS light (400–680 nm), 150 mW/cm <sup>2</sup>	For PNP: Complete removal in 30 min with simulated sunlight and 99% removal in 1.5 h with VIS light For TBBPA: 100% removal in 5 min with simulated sunlight and 98% removal with VIS light	[35]



Catalyst	Pollutant	Irradiation	Performance	Refs.
Cu <sub>2-x</sub> Se-g-C <sub>3</sub> N <sub>4</sub>	MB	500 W Xe lamp, $\lambda > 420$ nm	>95% removal in 2 h	[25]
Bi/I-coddecorated BiOIO <sub>3</sub>	Phenol, 2,4- DCP, BPA, RhB, TC	500 W Xe lamp VIS light ( $\lambda \geq 420$ nm) or simulated sunlight	With $\lambda \geq 420$ nm: 76.8% RhB removal in 4 h and >40% BPA removal in 5 h With simulated sunlight: 55% TC removal in 2h, 60% 2,4-DCP removal in 2 h, >90% phenol removal in 3 h	[24]
AgCl:Ag hollow nanocrystals	Reduction of Cr (VI) to Cr (III)	500 W Xe lamp, $\lambda \geq 420$ nm	100% of Cr (VI) photoreduced in 10 min (only 44.7% and 16.5% of Cr (VI) was reduced over AgCl-normal and commercial P25, respectively	[20]
SiO <sub>2</sub> -Au seeded nanoparticles	MO, TCE	Green laser $\lambda = 532$ nm	For MO, 61% removal by SiO <sub>2</sub> -Au seeded NPs and 29% removal by bare Au seeds after 1 h laser irradiation at 2 W For TCE, 50% removal after 1 h laser exposure at 2 W	[36]

BPA: Bisphenol A; CIP: ciprofloxacin; 4-CP: 4-Chlorophenol; 2,4-DCP: 2,4-Dichlorophenol; FA: Formic acid; FAD: Formaldehyde; GO: Graphene oxide; MB: methylene blue; MO: Methyl orange, PNP: P-nitrophenol; RGO: reduced graphene oxide; RhB: rhodamine B, TBBPA: tetrabromobisphenol-A; TC: tetracycline; TCE: Trichloroethylene, TP: titanium phosphate nanoplates; X-3B: reactive brilliant red.

**Table 1.** Recent studies on the utilization of plasmon-assisted photocatalysts for removal of aqueous contaminants.

Although most of plasmonic photocatalysts devoted to pollutants removal have been based on hybrid structures containing noble metals such as Au and Ag, supported on semiconductors (mostly TiO<sub>2</sub> or ZnO), novel plasmonic materials and structures are currently under development [21]. For instance, low-cost bismuth (Bi) has been reported to be an alternative to noble metals due to their direct plasmonic photocatalytic ability [22] which makes it a promising cocatalyst to enhance the efficiency of multiple photocatalysts, as reported in various recent studies [22–24]. Plasmonic semiconductor Cu<sub>2-x</sub>Se deposited on the surface of graphitic carbon nitride (g-C<sub>3</sub>N<sub>4</sub>) was also proposed as visible light photocatalysts for dye removal [25]. Recently, Meng and Zhang [26] developed and investigated for the first time a Pd-doped Bi<sub>2</sub>MoO<sub>6</sub> photocatalyst (Pd/PdCl<sub>2</sub>-Bi<sub>2</sub>MoO<sub>6</sub>) which exhibited an enhanced efficiency for phenol removal due to the reduction of electron-hole recombination rate, the SPR of Pd nanoparticles, and the generation of the strong oxidizing agent Cl<sup>0</sup> from Cl<sup>-</sup> on the surface of Bi<sub>2</sub>MoO<sub>6</sub>.

2.2. Organic synthesis

The application of heterogeneous photocatalysis in organic synthesis constitutes a more challenging issue than the degradation of organic contaminants [37] and much effort is being devoted in this field, as recently reviewed elsewhere [37–40]. The use of plasmonic nanomaterials as visible light-driven photocatalysts constitutes an interesting and appealing alternative to carry out a wide variety of chemical reactions to generate fine chemicals of industrial

interest while working under mild conditions [41]. This chapter section overviews some examples of representative reactions with both industrial and fundamental interests.

### 2.2.1. Oxidation reactions

The selective oxidation of alcohols to their corresponding carbonyl counterparts is one type of mostly studied plasmon-assisted photocatalyzed reactions [16]. For instance, Au/CeO<sub>2</sub> was applied for the selective oxidation of benzyl alcohols to corresponding benzaldehydes in aqueous suspensions under irradiation by visible light from a green LED [42]. Hallet-Tapley et al. [43] also demonstrated the ability of Au supported on hydrotalcite, ZnO, or Al<sub>2</sub>O<sub>3</sub> to selectively oxidize sec-phenethyl to acetophenone and benzyl alcohol to benzaldehyde, in presence of H<sub>2</sub>O<sub>2</sub> using 530 nm LED as the photoexcitation source (**Figure 4A**). Yu et al. [44] and more recently, Chen et al. [45] supported gold catalysts for the selective aerobic oxidation of benzyl alcohol to benzaldehyde driven by visible light. Plasmonic photocatalysis has also been applied to amide production via tandem oxidation/amidation processes catalyzed by Au/SiO<sub>2</sub> under 532 nm laser irradiation [46].

Esterification is one of the fundamental reactions in organic synthesis, as its products are widely used as precursors and intermediates for the production of fine chemicals, fragrances, natural products, or polymers [38]. Traditionally, esters are synthesized by the reaction of activated acid derivatives with alcohols, in multi-step reaction processes that yield high amounts of undesirable byproducts. In addition, these usually require harsh conditions of temperature, pressure, and pH [38, 47]. Xiao et al. [47] reported a one-pot process for the direct oxidative esterification of aliphatic alcohols under mild conditions, using gold-palladium alloy nanoparticles (Au-Pd alloy NPs) on a phosphate-modified hydrotalcite as a recyclable photocatalyst (**Figure 4B**). It was found that the intensity and wavelength of the irradiated light could remarkably change the reactivity. The explanation was that higher irradiance provides more light excited energetic electrons, resulting in a stronger electromagnetic field in the vicinity of the NPs (LSPR field enhancement effect). On the other hand, photons with a shorter wavelength (<550 nm) are able to excite metal electrons to higher energy levels, and these electrons have more chances to transfer to the antibonding orbitals and induce reaction. Wavelength effect is more important at low temperatures, when the excited electron transfer effect dominates the photocatalytic activity, and the thermal and photothermal effect contributes much less [47].

Likewise, Zhang et al. [48] reported the visible light driven esterification from aldehydes and alcohols using supported Au nanoparticles (Au/Al<sub>2</sub>O<sub>3</sub>) at ambient temperatures. From the results at different wavelength ranges, it is concluded that gold plays an active role in harvesting visible light and that the LSPR effect plays a critical role in enhancing the reaction activity in the catalyzed processes.

### 2.2.2. Reduction reactions

Chemical reduction reactions constitute another interesting route for the synthesis of fine chemicals, and plasmonic materials have also been utilized in several photocatalytic reduction

processes. For instance, plasmonic gold nanoparticles (Au NPs) were successfully applied as catalyst to perform the reduction of resazurin to resorufin [49] via laser drop (532 nm) or LED (530 nm) plasmon excitation. The use of Au NPs supported on different materials was also investigated for the selective reduction of organic compounds under visible light (or simulated sunlight) [50]. Au/CeO<sub>2</sub> catalysts were found to be efficient in the reduction of nitroaromatics to azocompounds, hydrogenation of azobenzene to hydroazobenzene, reduction of ketones to alcohols, and deoxygenation of epoxides to alkenes. The SPR effect of Au NPs was reported to play a key role in assisting activation of N=O bonds, so that the main product in the reduction of nitrobenzene under visible irradiation was different from that obtained under UV irradiation [50].

It has also been reported that Cu/graphene catalyst exhibits high activity for the reductive coupling of nitroaromatics to aromatic azocompounds under solar irradiation [51]. The product selectivity changed significantly with temperature, and conversion was found light intensity dependent. The light absorbed by Cu nanoparticles was the major driving force of the reaction as the highest conversion in the visible light range was in the range 530–600 nm, where the Cu nanoparticles strongly absorb the light due to the LSPR effect [52].

Another representative example is referred to the reduction of styrene in the presence of hydrogen to yield ethylbenzene. This chemical reduction was successfully achieved in the presence of Ag–Pd nanocages under visible light irradiation. In these photocatalysts, Pd provides active sites for hydrogenation reactions, whereas Ag offers plasmonic properties to convert light into heat [53].

### 2.2.3. Cross-coupling reactions

Plasmonic materials have also been investigated as photocatalysts for cross-coupling reactions, which have been accepted as convenient one-step methods to render complex molecules of interest for the synthesis of natural and advanced materials, bioactive products, agrochemicals, or medicines [38]. Au-Pd nanostructures consisting of Au nanocrystal cores and tightly bonded Pd nanoparticles could harvest visible to near-infrared (NIR) light for Suzuki coupling of iodobenzene or bromobenzenes and aromatic boronic acids to biphenyls under solar radiation, and also under 809 nm laser irradiation [54].

In a study by Xiao et al. [3], five different cross-coupling reactions, namely the Sonogashira, Stille, Hiyama and Ullmann C-C couplings, and the Buchwald-Hartwig amination (C-N cross-coupling) were investigated to demonstrate the possibility of applying Au-Pd alloy NP photocatalyst to enhance the intrinsic catalytic activity of Pd sites under visible light irradiation and at low temperatures (**Figure 4C**). The results suggest that electrons of alloy NP are excited under light irradiation and are then transferred from the nanoparticle surface to the reactant molecules adsorbed on the nanoparticle surface, weakening the chemical bonds of the molecules and facilitating the reactions. Increasing the light intensity accelerates the reaction rate due to increased population of photoexcited electrons. The irradiation wavelength also affected the reaction rates, and ultraviolet irradiation was required to drive some reactions with certain substrates.

Hu et al. [55] developed a novel and efficient approach to synthesize interfaced dimers made of Au NPs and bimetallic nanoshells, such as Au/Ag, Pt/Ag, or Pd/Ag. The Au NP-Pd/Ag bimetallic nanoshells were then used for catalyzing Suzuki coupling reactions between phenylboronic acid and iodobenzene at 80°C, yielding biphenyl. After 45 min in the dark, the conversion of reactants was 95%. Under visible light illumination, the reaction was significantly accelerated, 95% conversion in only 15 min. The increase in the reaction rate under illumination was attributed to the strong SPRs in the Au NPs, which enabled absorption of visible light in the dimers, leading to an enhancement in catalytic performance.

Cui et al. [56] synthesized  $\text{Cu}_7\text{S}_4\text{@Pd}$  heteronanostructures and probed their photocatalytic potential for Suzuki coupling reaction, hydrogenation of nitrobenzene, and oxidation of benzyl alcohol in the NIR range, respectively. As the  $\text{Cu}_7\text{S}_4\text{@Pd}$  LSPR peak position was close to 1500 nm, a 1500 nm diode laser was used as illumination source for the photocatalytic reactions. Additionally, irradiation at 808 and 980 nm were also evaluated. The highest conversions rates were obtained for 1500 nm irradiation due to LSPR enhancement in this region. To evaluate the pragmatic feasibility of the photocatalyst, the catalytic reactions were evaluated under real sunlight irradiation ( $\sim 40 \text{ mW/cm}^2$ ) as well, and high conversion rates were attained (Figure 4D).

In a study by Trinh et al. [7], plasmonic Pd hexagonal nanoplates, with tunable longitudinal LSPR were synthesized and applied to catalyze Suzuki coupling reaction. The catalytic activity of the Pd nanoplates was 2.5 and 2.7 times higher than that of nonplasmonic Pd nanooctahedral and Pd nanocubes, respectively, upon illumination at wavelengths in the range 300–1000 nm. These results, along with theoretical studies, revealed that Pd hexagonal nanoplates are able to harvest visible to NIR light, and that the increase in the catalytic activity on Pd nanoplates is primarily a result of the plasmonic photocatalytic effect of plasmon-induced hot electrons. Recently, it has been revealed that metal oxide nanostructures, such as  $\text{WO}_{3-x}$ ,  $\text{MoO}_{3-x}$ , and  $\text{TiO}_{2-x}$ , can exhibit LSPR in the visible and NIR region due to abundant oxygen vacancies or heavy doping [57, 58]. Lou et al. [57] demonstrated that the plasmon excitation of  $\text{WO}_{3-x}$  nanowires by long wavelength irradiation can enhance main product yield and selectivity in Suzuki coupling reactions catalyzed by the attached Pd nanoparticles.

### 2.3. Disinfection

While  $\text{TiO}_2$  photocatalytic inactivation of bacteria and viruses has been known for decades [59], the number of studies using plasmonic materials for water disinfection is still rather limited.

Silver halides ( $\text{Ag/AgX}$  where  $\text{X} = \text{Cl, Br, I}$ ) supported on  $\text{TiO}_2$  or carbon materials have been the most studied photocatalysts for antimicrobial applications. Tian et al. [60] prepared a  $\text{AgCl@Ag@TiO}_2$  sandwich-structured photocatalyst and evaluated its bactericidal activities in terms of the inactivation of Gram-negative bacteria *Escherichia coli* K12 (*E. coli* K12) under visible light irradiation. In the absence of irradiation, the catalyst exhibited a negligible killing response, whereas visible light irradiation in absence of photocatalyst only achieved the inactivation of 6% *E. coli* colonies in 30 min. In contrast, when  $\text{AgCl@Ag@TiO}_2$  was used, nearly 77% of *E. coli* K12 population was inactivated after 6 min under



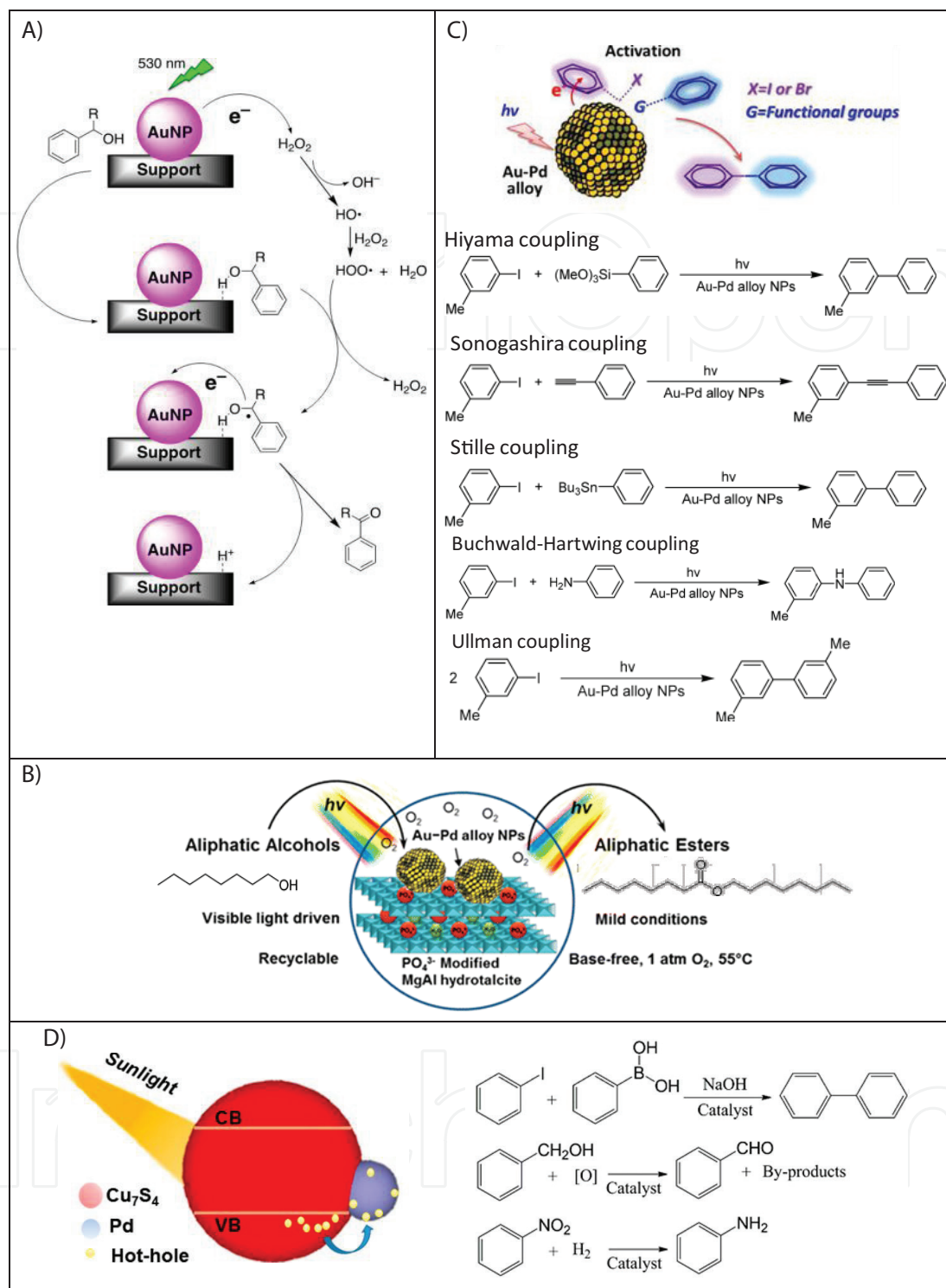


**Figure 4.** (A) Proposed mechanism for the plasmon-mediated oxidation of sec-phenethyl ( $R = \text{CH}_3$ ) and benzyl ( $R = \text{H}$ ) alcohols in the presence of supported AuNP. Reprinted with permission from Ref. [43]. Copyright (2013) American Chemical Society. (B) Direct oxidative esterification of aliphatic alcohol (1-octanol as example). Adapted with permission from Ref. [47]. Copyright (2015) American Chemical Society. (C) Scheme of cross-coupling reactions catalyzed by Au-Pd alloy NPs under visible light irradiation. Adapted with permission from Ref. [3]. Copyright (2014) American Chemical Society. (D) Schematic representation of plasmon enhanced Suzuki coupling reaction, oxidation of benzyl alcohol and hydrogenation of nitrobenzene, over  $\text{Cu}_7\text{S}_4/\text{Pd}$  heteronanostructures. Reprinted with permission from Ref. [56]. Copyright (2015) American Chemical Society.



visible light irradiation, reaching total inactivation at 15 min. Under visible light irradiation, Ag NPs produce electrons and holes, which can be separated by the SPR-induced local electromagnetic field. Due to the suitable conduction band and valence band energy levels of AgCl and TiO<sub>2</sub>, the photo-generated electrons transfer to TiO<sub>2</sub> while holes transfer to AgCl. The electrons are trapped by adsorbed O<sub>2</sub> to form  $\cdot\text{O}_2^-$ , while the holes combine with OH<sup>-</sup>/or Cl<sup>-</sup> ions to form  $\cdot\text{OH}$ /or Cl<sup>0</sup> radicals. All of  $\cdot\text{O}_2^-$ ,  $\cdot\text{OH}$ , and Cl<sup>0</sup> radicals are reactive species responsible for the inactivation of bacteria. Simultaneously, Shi et al. [61] studied the photocatalytic inactivation of *E. coli* by Ag/AgX-CNTs under visible light. The Ag/AgBr-CNTs exhibited an excellent photocatalytic disinfection performance, achieving the complete inactivation of  $1.5 \times 10^7$  cfu/mL of *E. coli* within 40 min. This was attributed to the SPR of Ag nanoparticles and the efficient photo-generated carrier separation owing to the CNTs. Thus, a high concentration of electrons migrates to the surface of CNTs, where they can be trapped by O<sub>2</sub> and H<sub>2</sub>O to produce  $\cdot\text{O}_2^-$  and H<sub>2</sub>O<sub>2</sub>.



These species, along with  $\cdot\text{OH}$  produced from holes in the surface of AgBr, are involved in the photocatalytic bacterial inactivation process.

More recently, Xia et al. [62] prepared a series of Ag/AgX/RGOs (RGO = reduced graphene oxide) composites and evaluated their performance for water disinfection upon visible light. The visible light irradiation without plasmonic catalyst or the photocatalyst in the absence of light irradiation showed no bactericidal effect. Upon visible light irradiation, Ag-AgBr/RGO exhibited high photocatalytic inactivation efficiency and attained complete inactivation of 7 log cfu/mL *E. coli* cells in 8 min. Remarkably, additional experiments were also carried out to evaluate the possible effect of Ag<sup>+</sup> ions in order to clarify the disinfection mechanism of Ag-based plasmonic photocatalyst. Authors found that light irradiation promoted the release of free Ag<sup>+</sup> ions from Ag-AgBr/RGO and also enhanced the antimicrobial activities of Ag<sup>+</sup> ions. These were able to induce the damage of metabolic process while the cell membrane damage was rather limited. The primary bactericidal effect of visible light irradiated Ag-AgBr/RGO resulted from the sustainable generation of reactive species. Plasmonic-induced H<sub>2</sub>O<sub>2</sub> plays the leading role, collaborating with e<sup>-</sup>,  $\cdot\text{O}_2^-$ ,  $\cdot\text{OH}$  to induce damage of microbial metabolism processes, destroy the cell envelope and lead to the leakage and degradation of intracellular substances.

AuNP-based nanocomposites have also been investigated for disinfection applications. In this regard, Sarkar et al. [63] developed a plasmonic photocatalyst derived from functionalized amylopectin and *in situ* incorporated TiO<sub>2</sub> and AuNPs (g-AP-pAA/TiO<sub>2</sub>-Au), and demonstrated its antimicrobial activity in the presence of both UV, and especially, visible light irradiation, as depicted in **Figure 5**.

Li et al. [64] developed a nonnoble metal plasmonic photocatalyst consisting of a TiN/TiO<sub>2</sub> composite and evaluated its performance for the photocatalytic disinfection of *E. coli* in a buffer solution under visible light illumination. In the absence of photocatalyst or visible light,

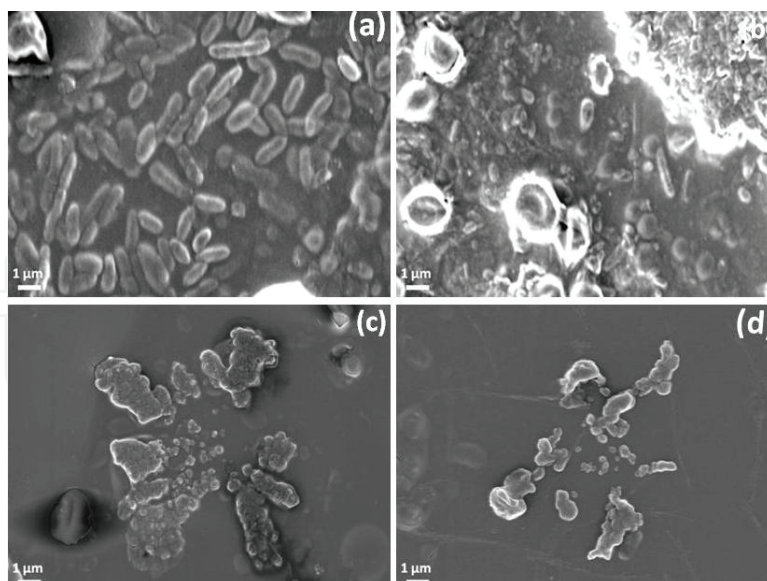


**Figure 5.** Field emission scanning electron microscopes images of *E. coli* (a) in absence of light source; (b) in presence of UV light; (c) in presence of g-AP-pAA/TiO<sub>2</sub> along with UV light; and (d) in presence of g-AP-pAA/TiO<sub>2</sub>-Au along with visible light. Reprinted with permission from Ref. [63]. Copyright (2016) American Chemical Society.

the survival ratio of *E. coli* population showed no obvious change. In the presence of TiN/TiO<sub>2</sub> photocatalyst under illumination ( $\lambda > 400$  nm), the survival ratio of *E. coli* colonies dropped continuously upon increasing irradiation times. According to the proposed mechanism, TiN nanostructures constitute the plasmonic component in the composite to harvest visible light and generate hot electrons by the LSPR effect. These hot electrons, once they were excited above the Fermi energy level of TiN, could be injected quickly into the conduction band of TiO<sub>2</sub>, to react with O<sub>2</sub> yielding  $\cdot\text{O}_2^-$  and subsequently  $\cdot\text{OH}$ , which are able to disinfect microorganisms.

### 3. Nanoplasmonic photocatalysis in gas-phase reactions

Besides their use in aqueous media photocatalysis, plasmonic nanomaterials have been lately investigated for their use in gas-phase reactions. Due to the broad range of reactions in gas phase currently under study, in this section we will focus on two big groups of them: degradation of volatile organic compounds (VOCs) and chemical to energy conversion.

#### 3.1. Photo-degradation of volatile organic compounds

Air pollution is of great concern nowadays due to the damage that a long exposure can do to human health. Indoor and outdoor environments are suitable to suffer from high concentration of VOCs due to human activity, so currently it is considered urgent to address this problem in a more efficient way. Currently, the methods used to eliminate VOCs vary from physical methods like filtration or adsorption, to chemical ones like UV irradiation or

ozone treatment [65]. The latter, being efficient for the purpose of eliminating the hazardous materials from air, is also harmful to human health, so there is a need for new methods to eliminate VOCs from air. In this case, the use of plasmonic materials seems to be a logical step forward, not only in order to avoid exposure to dangerous atmospheres, but also because of the possibility of using solar energy instead of other expensive and unsafe source of energy. While the examples of photocatalysis for VOCs elimination are growing lately, the ones using plasmonic materials, even when growing every year, are still far from conventional semiconductors ones. One of the first examples in using plasmonic materials for VOCs remediation comes from Chen et al. [66]. They used Au NPs supported in different metal oxides to get the total oxidation of formaldehyde with visible light. In this case, the authors wanted to use a pure plasmonic material, so they attached the Au NPs to oxide supports like  $\text{ZrO}_2$  or  $\text{SiO}_2$ , both with high band gap (5 and 9 eV, respectively) in order to avoid excitation of the support from the visible light source. The mechanism proposed involves two of the features of plasmonic materials mentioned above. In one hand, irradiating the Au NPs on their plasmon band will increase the temperature locally high enough to perform the VOCs oxidation in high extent. Besides the temperature effect, the high electric field generated on the surface of the nanoparticles would activate polar molecules as formaldehyde present on the surface of Au NPs, aiding to the total oxidation of the compound. Another example of decomposition of VOCs using plasmonic materials is the isopropanol oxidation performed by Dinh et al. [67]. In this case, the structure of the catalyst is a key for its performance. It consists of Au/ $\text{TiO}_2$  nanostructured photocatalyst that is constructed by the three-dimensional ordered assembly of thin-shell Au/ $\text{TiO}_2$  hollow nanospheres. Due to that composition, it can be considered a hybrid plasmonic structure with some special qualities. The authors claim that the photonic structure of the catalyst enhances the absorption of the plasmonic AuNP by the multiple scattering and the slow photon effect characteristic of these architectures. This enhancement absorption of the plasmon band provides an activity several times higher than the normal Au/ $\text{TiO}_2$  structure.

The last example for VOCs oxidation using plasmonic materials comes from Sellappan et al. [68]. They combine gold and silver nanoparticles with  $\text{TiO}_2$  with different configurations in order to evaluate the electron transfer after light excitation. They evaluate the photocatalysis of the degradation of methanol and ethylene under different conditions. One of those conditions is the physical contact between the metal and the semiconductor. When the nanoparticles are in contact with  $\text{TiO}_2$ , a Schottky barrier is formed, which enhances the charge separation under UV light illumination. When the metals are not in contact with the support, they also observe an enhancement in the activity of the photocatalyst that they assign to a near and far field effect of the plasmonic nanomaterial. This is so because, even when they are separated, the distance is short enough from the support to feel the high electric field generated on the metal nanoparticle.

### 3.2. Plasmonic-driven chemical to energy conversion processes

Global warming is nowadays one of the biggest problems to be addressed in our society. The vast amount of fossil fuel consumed during the last decades has broken the natural balance

of CO<sub>2</sub> emission and uptake, leading to high concentrations of this gas in the atmosphere and in the oceans, and provoking a sharp climate change. Besides, due to this enormous growing in fossil fuel consumption, the society is exhausting their reserves at a very high rate creating an urgent need for alternative sources of energy. With this in mind, photocatalysis has emerged as a promising tool to kill two birds with one stone. On one hand, it can help to reduce the CO<sub>2</sub> emitted to the atmosphere and also in that process give products that could be able to store energy. As a first example of this, in 1979 Inoue et al. [69] attained for the first time the reduction of CO<sub>2</sub> with light using several semiconductors as photocatalysts. Even when the reaction was performed in liquid phase, we consider appropriate to mention it here since it was the first attempt that obtained valuable products after the reduction of CO<sub>2</sub> using light as energy source. Since that first work, many attempts have been made in order to synthesize photocatalysts to reduce CO<sub>2</sub> to different interesting products. Most of those catalysts are semiconductors like TiO<sub>2</sub> or ZnO which, while they possess many interesting properties to be used as photocatalysts, they also have some drawbacks that limit their use on large scale applications, as low photon absorption efficiency, high charge carrier recombination rate or being restricted to the UV region of the spectra. In order to overcome these downsides, in recent years the scientific community have paid attention to plasmonic materials as an attractive tool to be used for the reduction of CO<sub>2</sub>. Liu et al. [70] first reported the use of plasmonic gold catalyst for the dry reforming of CO<sub>2</sub> with methane to obtain syngas. This reaction usually requires high temperatures (800–1000°C) and is of great interest since it would transform two greenhouse gases into molecules suitable for energy storage like CO and H<sub>2</sub>. They prepared a catalyst consisted of Rh and Au supported on SBA-15 in order to use the good properties of Rh for this reaction and the plasmon band of Au to activate the reactants. They claim that the high electric field generated on the AuNP induces polarization on the CO<sub>2</sub> and the CH<sub>4</sub> molecules activating them, and enhances the conversion to syngas. Another interesting reaction involving the consumption of CO<sub>2</sub> is the reverse water gas shift reaction (RWGS). Upadhye et al. [71] probed that using AuNP supported over TiO<sub>2</sub> and CeO<sub>2</sub>, they could enhance the yield of the reaction illuminating with visible light from 30 to 1300%. According to them, the LSPR of the catalyst changed the intrinsic kinetics of the reaction on the surface of the catalyst by increasing the rate constant of either the carboxyl decomposition or the hydroxyl hydrogenation, two of the key steps in this reaction. They attributed the rate enhancement either to the generation of hot electrons or the polarization effect of the high electric field generated by the plasmonic nanoparticles on the adsorbates. Not only conventional semiconductor materials have been used to support plasmonic nanoparticles, lately several authors have used graphene and derivative as active supports for photocatalysis. This is the case of Shown et al. [72] that evaluated the activity of Cu NPs supported on graphene oxide (GO) for the reduction of CO<sub>2</sub> (**Figure 6**). In their work, they prepared the catalyst with different Cu loading and evaluated the photoreduction using visible light, and compared the results with GO alone and with TiO<sub>2</sub> P25. The authors found an increase in the products yield for the CuGO hybrid material by 60 times with respect to the GO, and 240 times with respect to the P25, obtaining methanol and acetaldehyde as the main products. They attributed the enhancement to a modification in the work function of the GO by the Cu NPs that improved the charge separation.



Finally, some additional examples where  $\text{CO}_2$  has been successfully hydrogenated to yield methane in the presence of nanoplasmonic photocatalysts are briefly described below and summarized in **Table 2**. Methane has gained an increasing interest, given its abundance and its extended use as fuel in fertilizers or as intermediate in the petrochemical industry [73]. Most of the studies report the combination of titania or P25 semiconductor supports with noble-metal-based cocatalysts, which are able to expand the band gap toward the visible range through their surface plasmon band [74], act as charge reservoirs, and also as active and selective catalytic centers [74–81]. In this regard, the presence of Pd or Pt strongly enhances the selectivity toward methane in comparison with the preferential pathway toward CO observed in  $\text{TiO}_2$ , being of paramount importance for the proper formation of organic intermediates. As a major drawback, progressive deactivation was observed upon oxidation of Pd into PdO domains [79]. Furthermore, the effective formation of Au-Cu alloys was also found extremely active, thereby outperforming the photo-

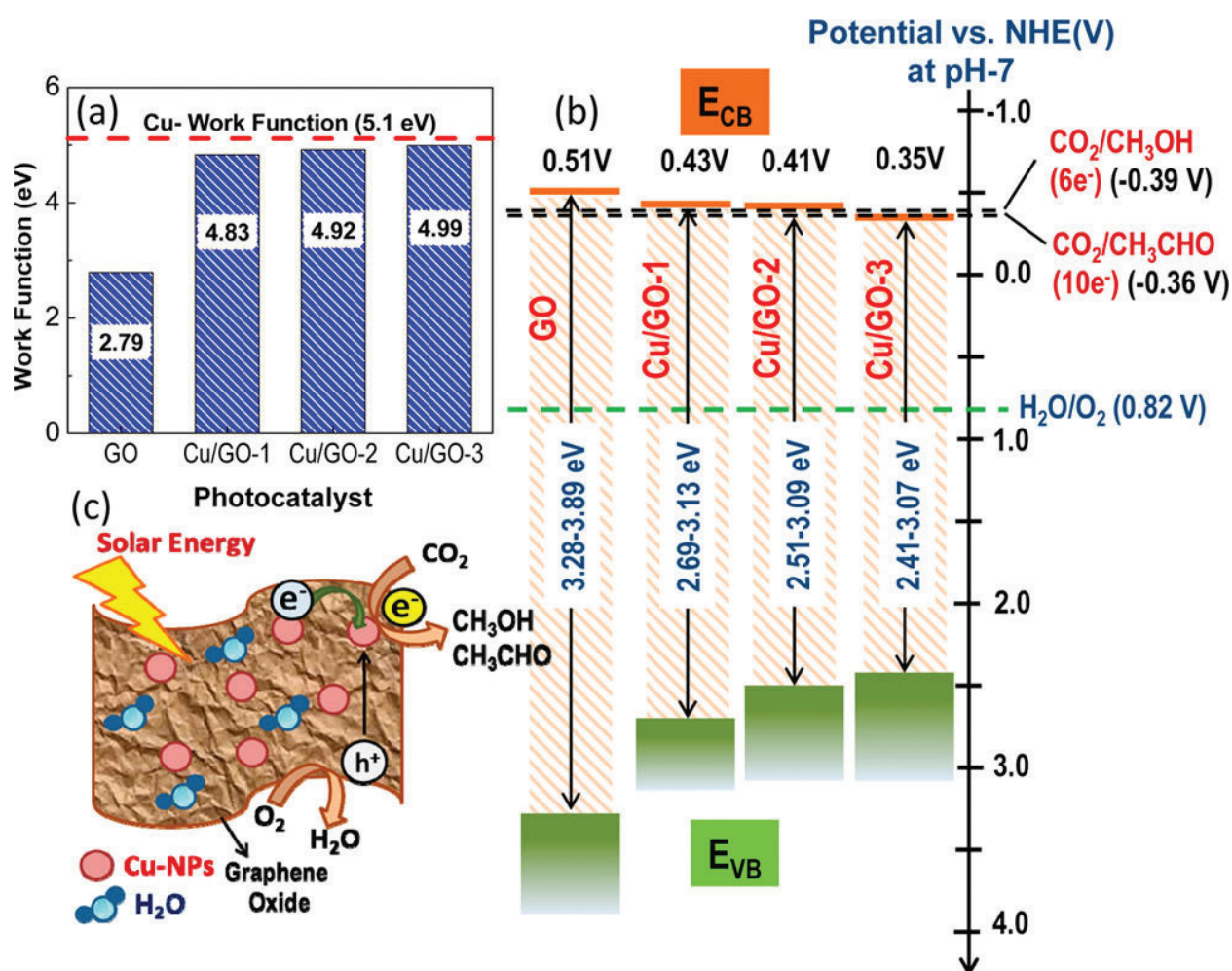


**Figure 6.** (a) UPS-determined work functions of GO and Cu/GO hybrids and (b) band-edge positions of pristine GO and Cu/GO hybrids as compared with  $\text{CO}_2/\text{CH}_3\text{OH}$  and  $\text{CO}_2/\text{CH}_3\text{CHO}$  formation potential. (c) Schematic photocatalytic reaction mechanism. Reprinted with permission from Ref. [72]. Copyright (2015) American Chemical Society.



catalytic conversions of their respective single metal counterparts, while expanding their response in the visible range as nicely demonstrated by transient absorption spectroscopy studies [74].

Other relevant studies additionally dealt with the use of catalytic monoliths [75], fluidized-bed reactors combined with LEDs [77] or included the use of novel semiconductor supports based on carbon nitride or reduced graphene oxide that provided additional sites for the accommodation of CO<sub>2</sub> and the active cocatalysts [76, 82]. Finally, Zhang et al. synthesized a hybrid material consisted of Rh nanocubes supported on Al<sub>2</sub>O<sub>3</sub> and used for the selective hydrogenation of CO<sub>2</sub> to CH<sub>4</sub>, avoiding almost completely the competitive production of CO (see **Figure 7**). The authors used UV and blue light coming from LED irradiators in order to excite the plasmon band of the metal nanoparticles and generate high-energy electrons that are transferred to the adsorbates [81].

Catalyst	Reductant	Cocatalyst	Remarks	Refs.
Au, In/TiO <sub>2</sub>	H <sub>2</sub>	Au, In	Irradiation with UV lamp (200 W; 150 mW/ cm <sup>2</sup> ) Use of monolithic reactors	[75]
Pd/TiO <sub>2</sub>	H <sub>2</sub> O	Pd	Irradiation with UV-LED arrays (40 pieces) (365 nm) Fluidized bed reactors + T = 140°C	[77]
Pd/TiO <sub>2</sub>	H <sub>2</sub> O	Pd	Irradiation at λ > 310 nm Formation of organic adsorbates is critical	[79]
Core-shell Pt/TiO <sub>2</sub> PtCu/TiO <sub>2</sub>	H <sub>2</sub> O	Cu, Pt	Light source 780 > λ > 320 nm Strong influence of cocatalysts on selectivities	[80]
Au,Cu/P25	H <sub>2</sub> O	Au, Cu, Au-Cu alloys	λ= 355 and 532 nm Performance of transient absorption experiments	[74]
Ternary composition Metal + RGO + TiO <sub>2</sub>	H <sub>2</sub> O	Pt, Pd, Ag, Au	Visible light irradiation (energy daylight bulb, 15 W) Pt-doped showed best activity	[76]
Ag(AgCl)- Carbon Nitride	H <sub>2</sub> O	-	In situ generation of Ag plasmonic domains 400 < λ < 650 nm 30 fold enhancement with P25	[82]
Rh cubes/Al <sub>2</sub> O <sub>3</sub> Au/Al <sub>2</sub> O <sub>3</sub>	H <sub>2</sub>	–	Irradiation with UV, blue and white LEDs Comparison with thermal reaction	[81]

**Table 2.** Summary of selected photocatalysts for conversion of CO<sub>2</sub> into CH<sub>4</sub>.

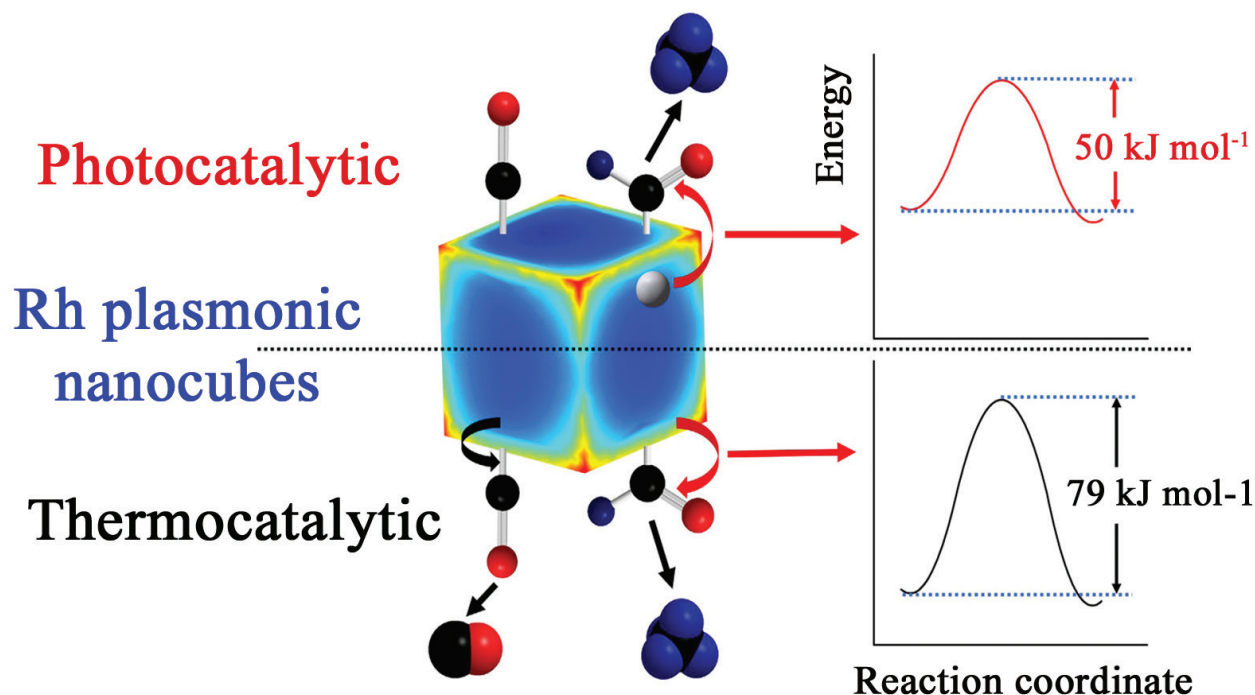


**Figure 7.** Representative example of recently developed plasmonic catalysts for the CO<sub>2</sub> hydrogenation into methane: Reaction mechanism on Rh nanocube comparing the preferential activation of CO in the thermocatalytic process in contrast to the methane pathway favored under photocatalytic conditions. Adapted with permission from Ref. [81]. Copyright (2017) Nature Publishing Group.

## 4. Plasmonics in biocatalytic processes

### 4.1. Photobiocatalysis

A promising field for the use of nanoplasmonics currently under development is the photobiocatalysis. In this relatively novel area, the main goal is obtaining photocatalysts inspired in natural photosynthetic centers. A brief overview of the current state of the art in this field devoted to regular semiconductors has been recently published elsewhere [83]. More recent studies involving the use of plasmonic materials have been reported by Sanchez-Iglesias et al. Their studies focused on the evaluation of multiple gold-shaped plasmonic nanostructures (see **Figure 8**) and their effect on the effective photoregeneration of nicotinamide adenine dinucleotide (NADH) molecules. These latter molecules are extremely important in natural biochemical routes as mediating cofactors in many enzymes [84, 85]. Moreover, cofactor molecules are necessary, for instance, in the photosynthesis process as light harvesters and intervening in the reduction-oxidation balances involved in respiration [86]. The major drawbacks associated with cofactor molecules have arisen from the limited success achieved in the past year attempting their regeneration (reduction) via nonenzymatic pathways. Organic dyes, semiconductors, or polymers have been previously used as photocatalysts to regenerate NADH cofactors, but these molecules intrinsically possess a poor quenching ability to accept electrons. Therefore, the need for implementing an electron relays acting as mediator

has been suggested to overcome this limitation. Up to date, the choice of suitable mediators has been rather scarce and limited to a few examples of Rh-based organometallic complexes. The use of gold plasmonic nanostructures represents a more straightforward and affordable alternative.

The first successful example of plasmonic cofactor photoregenerator was reported for gold nanorods coated with Pt domains on their tips (**Figure 8B**), thereby representing a previously defined plasmonic photocatalyst containing a heterojunction that combines a plasmonic structure (Au NRs) and a catalytic active site (Pt) to successfully carry out the regeneration (reduction) of NADH cofactor molecules [85]. A subsequent study carried out by the same authors determined an even more remarkable photo-response of gold nanostars with epitaxially grown Pt domains that was associated to the major light harvesting capacity of the star-shaped plasmonic structures (see **Figure 8A**) [84, 85]. The potential combination of these plasmonic heterojunctions with other semiconductors represents a very promising alternative to obtain suitable mediators that can help to modulate multiple biochemical processes via light-induced inputs.

#### 4.2. Artificial enzymes

Another niche of great biotechnological interest for the potential application of nanoplasmonics is related with the search for novel artificial enzymes [86]. Natural enzymes are well-known biocatalysts that regulate every biochemical processes involving living organisms. Recently, an emerging research subfield has emerged to find novel nanomaterials that can mimic the role of natural enzymes as highly active, and specific catalysts without incurring in

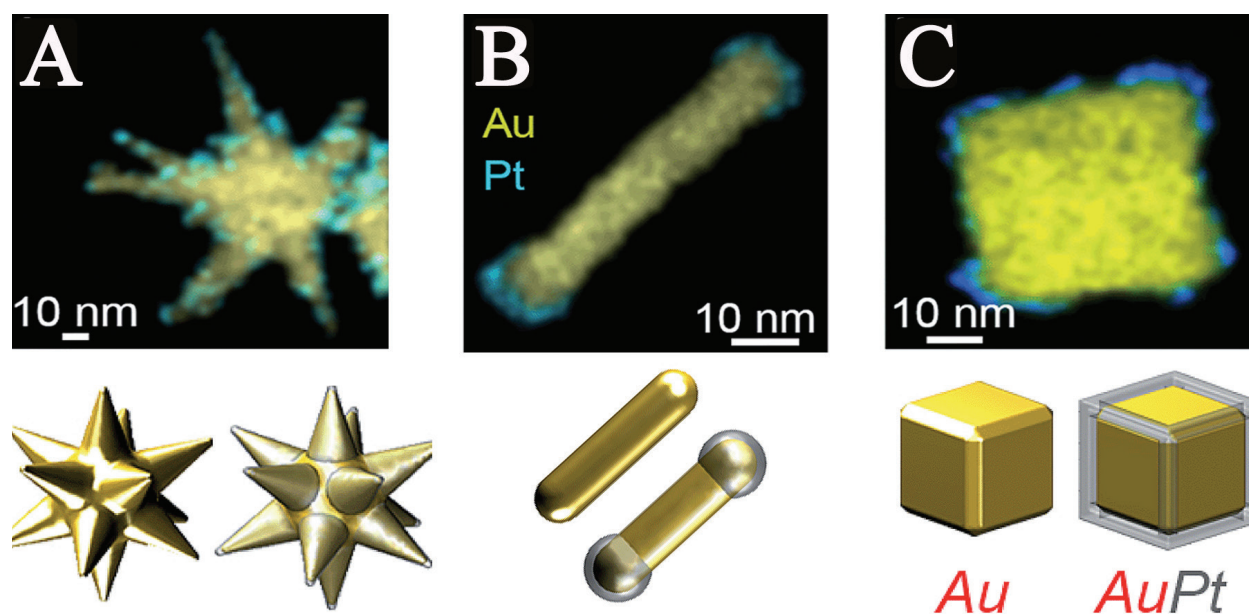


**Figure 8.** STEM-EDX analysis of Pt-decorated gold nanoplasmonics with different shapes and corresponding 3D models used for photoregeneration of NADH cofactor molecules: (A) stars; (B) nanorods; and (C) nanocubes. Adapted from Refs. [84, 85] with permission of The Royal Society of Chemistry.

their intrinsic limitations, such as limited stability by denaturalization, strong sensibility on variations of their optimal environment, difficulties for effective retrieval and reuse, and high costs derived from the multiple synthesis and purification steps implied in their preparation. In order to circumvent these major drawbacks, the search for stable and affordable alternatives has brought the spotlight on the development of artificial systems based on inorganic/organic nanomaterials.

In this regard, it is worth mentioning that Prof. Santamaria's group recently developed and tested one of the first NIR-activated enzyme-like plasmonic photocatalysts used as a glucose-oxidase surrogate (**Figure 9**) [87]. Glucose-oxidase biomimetic systems hold a huge potential for biomass conversion, selective detection of glucose in blood at trace levels, and control/monitoring of internal metabolism in cells. Previous candidates based on photocatalytic semiconductors such as  $\text{TiO}_2$  or  $\text{ZnO}$  rendered promising photoconversion of glucose [88, 89], but the combination of plasmonic gold nanorods cores holding excellent NIR absorption capabilities with an outer titania nanoshell proposed by Ortega-Liebana et al. provided not only an extended response toward the whole visible-NIR range, but also additional thermal stability and photoactivity toward the effective and preferential oxidation of glucose into gluconic acid and hydrogen peroxide (**Figure 9**). In addition, the activity of these core-shell nanostructures was maintained in a wide pH range and was effective at near room temperature. The authors claimed that the minimal thickness of the  $\text{TiO}_2$  shell ensured the formation of an effective Schottky barrier at the interface between Au and  $\text{TiO}_2$ . It was also remarkable to find out that the uncoated Au NRs exhibited negligible photo-response toward the glucose oxidation, thereby corroborating the need of the semiconductor titania shell fraction to promote the generation of active radicals and the selective oxidation of the sugar molecules [87].

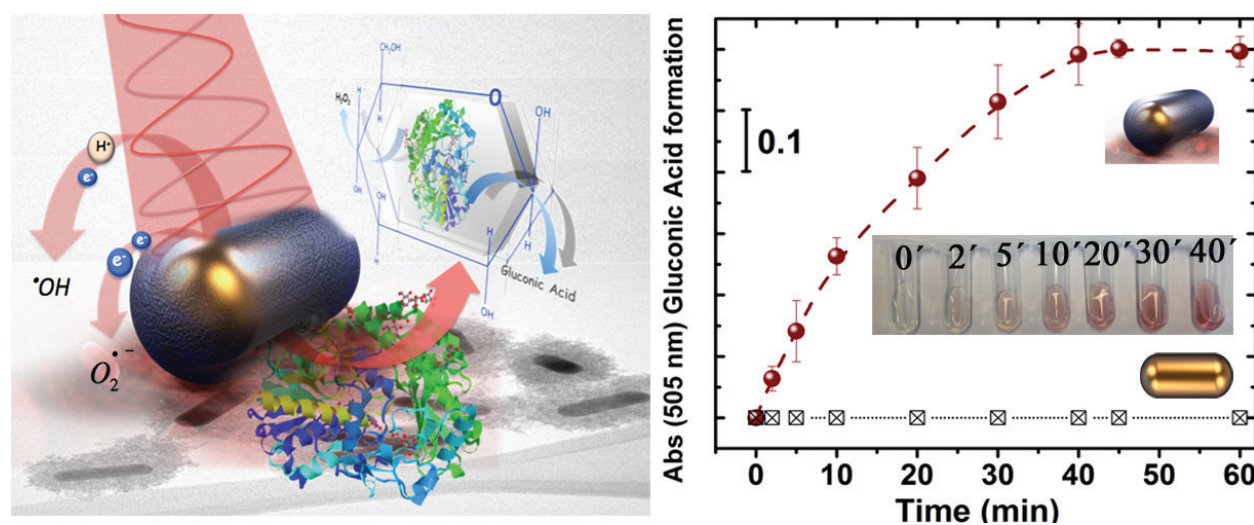


**Figure 9.** (Left) Schematic plot displaying the glucose-oxidase mimetic action of the titania-coated gold nanorods plasmonic photocatalyst under NIR irradiation; (Right) Colorimetric detection of the glucose when selectively converted into gluconic acid via the formation of a Fe-hydroxamate complex. Uncoated Au-NRs exhibit negligible photooxidation properties in comparison with the coated ones. Photocatalytic experiments were carried out with an 808 nm laser. Partially reprinted with permission from Ref. [87].



## 5. Conclusions

Plasmonic-based nanomaterials hold a very promising future as potential alternatives for the fabrication of next generation photocatalysts and processes where the wavelength irradiation range is expanded toward the visible and near-infrared windows, thereby maximizing the use of the solar irradiation. A wide variety of fields of action can be foreseen including those described in the present chapter and some additional options including the generation of biofuels from water or biomass, photoelectrocatalysis, solar cells, or photovoltaics. The use of these types of catalysts for light-triggered therapy treatments and the specific targeting for cell-mechanisms can also be envisioned as another promising area of expansion. In conclusion, the use of plasmonics is likely going to emerge with abundant and interesting breakthroughs in the next future.

## Acknowledgements

The authors acknowledge the European Research Council for funding through an advanced grant research project (HECTOR-267626) and a CIG-Marie Curie Reintegration Grant (NANOLIGHT-REA 294094). The Spanish Ministry of Economy, Industry and Competitiveness is also gratefully acknowledged (project CTQ2016-77147-R). C.B.A. and A.A.R. also thank the Spanish Government and the Juan de la Cierva program for two postdoctoral fellowships. CIBER-BBN is an initiative funded by the VI National R&D&I Plan 2008-2011 financed by the Instituto de Salud Carlos III with assistance from European Regional Development Fund.

## Author details

Carlos J. Bueno-Alejo<sup>1,2</sup>, Adriana Arca-Ramos<sup>1,2,3</sup> and Jose L. Hueso<sup>1,2,3\*</sup>

\*Address all correspondence to: jlhueso@unizar.es

1 Institute of Nanoscience of Aragon, University of Zaragoza, Zaragoza, Spain

2 Department of Chemical Engineering and Environmental Technology, University of Zaragoza, Zaragoza, Spain

3 Networking Research Center on Bioengineering, Biomedical and Nanomedicine, CIBER-BBN, Madrid, Spain

## References

- [1] Zou ZG, Ye JH, Sayama K, Arakawa H. Direct splitting of water under visible light irradiation with an oxide semiconductor photocatalyst. *Nature*. 2001;**414**(6864):625-657. DOI: 10.1038/414625a



- [2] Li XH, Zhu JM, Wei BQ. Hybrid nanostructures of metal/two-dimensional nanomaterials for plasmon-enhanced applications. *Chemical Society Reviews*. 2016;**45**(14):3145-3187; correction 2016;**45**(14):4032. DOI: 10.1039/c6cs90055k
- [3] Xiao Q, Sarina S, Bo AX, Jia JF, Liu HW, Arnold DP, et al. Visible light-driven cross-coupling reactions at lower temperatures using a photocatalyst of palladium and gold alloy nanoparticles. *Acs Catalysis*. 2014;**4**(6):1725-1734. DOI: 10.1021/cs5000284
- [4] Fasciani C, Alejo CJB, Grenier M, Netto-Ferreira JC, Scaiano JC. High-temperature organic reactions at room temperature using plasmon excitation: Decomposition of dicumyl peroxide. *Organic Letters*. 2011;**13**(2):204-207. DOI: 10.1021/ol1026427
- [5] Hallett-Tapley GL, Silvero MJ, Gonzalez-Bejar M, Grenier M, Netto-Ferreira JC, Scaiano JC. Plasmon-Mediated catalytic oxidation of sec-phenethyl and benzyl alcohols. *Journal of Physical Chemistry C*. 2011;**115**(21):10784-10790. DOI: 10.1021/jp202769a
- [6] da Silva AGM, Rodrigues TS, Correia VG, Alves TV, Alves RS, Ando RA, et al. Plasmonic nanorattles as next-generation catalysts for surface plasmon resonance-mediated oxidations promoted by activated oxygen. *Angewandte Chemie-International Edition*. 2016;**55**(25):7111-7115. DOI: 10.1002/anie.201601740
- [7] Trinh TT, Sato R, Sakamoto M, Fujiyoshi Y, Haruta M, Kurata H, et al. Visible to near-infrared plasmon-enhanced catalytic activity of Pd hexagonal nanoplates for the Suzuki coupling reaction. *Nanoscale*. 2015;**7**(29):12435-12444. DOI: 10.1039/c5nr03841c
- [8] Liu Z, Huang YM, Xiao Q, Zhu HY. Selective reduction of nitroaromatics to azoxy compounds on supported Ag-Cu alloy nanoparticles through visible light irradiation. *Green Chemistry*. 2016;**18**(3):817-825. DOI: 10.1039/c5gc01726b
- [9] Fujishima A, Honda K. Electrochemical photolysis of water at a semiconductor electrode. *Nature*. 1972;**238**(5358):37-38. DOI: 10.1038/238037a0
- [10] Manthiram K, Alivisatos AP. Tunable localized surface plasmon resonances in tungsten oxide nanocrystals. *Journal of the American Chemical Society*. 2012;**134**(9):3995-3998. DOI: 10.1021/ja211363w
- [11] Huang QQ, Hu S, Zhuang J, Wang X. MoO<sub>3-x</sub>-based hybrids with tunable localized surface plasmon resonances: Chemical oxidation driving transformation from ultrathin nanosheets to nanotubes. *Chemistry-A European Journal*. 2012;**18**(48):15283-15287. DOI: 10.1002/chem.201202630
- [12] Yan JQ, Wang T, Wu GJ, Dai WL, Guan NJ, Li LD, et al. Tungsten oxide single crystal nanosheets for enhanced multichannel solar light harvesting. *Advanced Materials*. 2015;**27**(9):1580-1586. DOI: 10.1002/adma.201404792
- [13] Zhang YW, Tian JQ, Li HY, Wang L, Qin XY, Asiri AM, et al. Biomolecule-assisted, environmentally friendly, one-pot synthesis of CuS/Reduced graphene oxide nanocomposites with enhanced photocatalytic performance. *Langmuir*. 2012;**28**(35):12893-12900. DOI: 10.1021/la303049w

- [14] Ibhaddon A, Fitzpatrick P. Heterogeneous photocatalysis: Recent advances and applications. *Catalysts*. 2013;**3**(1):189
- [15] Herrmann J-M. Heterogeneous photocatalysis: Fundamentals and applications to the removal of various types of aqueous pollutants. *Catalysis Today*. 1999;**53**(1):115-129. DOI: [http://dx.doi.org/10.1016/S0920-5861\(99\)00107-8](http://dx.doi.org/10.1016/S0920-5861(99)00107-8)
- [16] Jiang R, Li B, Fang C, Wang J. Metal/semiconductor hybrid nanostructures for plasmon-enhanced applications. *Advanced Materials*. 2014;**26**(31):5274-5309. DOI: 10.1002/adma.201400203
- [17] Fan W, Leung MKH, Yu JC, Ho WK. Recent development of plasmonic resonance-based photocatalysis and photovoltaics for solar utilization. *Molecules*. 2016;**21**(2):pii: E180. DOI: 10.3390/molecules21020180
- [18] Xiao M, Jiang R, Wang F, Fang C, Wang J, Yu JC. Plasmon-enhanced chemical reactions. *Journal of Materials Chemistry A*. 2013;**1**(19):5790-5805. DOI: 10.1039/C3TA01450A
- [19] Meng X, Zhang Z. Synthesis and characterization of plasmonic and magnetically separable Ag/AgCl-Bi<sub>2</sub>WO<sub>6</sub>@Fe<sub>3</sub>O<sub>4</sub>@SiO<sub>2</sub> core-shell composites for visible light-induced water detoxification. *Journal of Colloid and Interface Science*. 2017;**485**:296-307. DOI: 10.1016/j.jcis.2016.09.045
- [20] Li H, Wu T, Cai B, Ma W, Sun Y, Gan S, et al. Efficiently photocatalytic reduction of carcinogenic contaminant Cr(VI) upon robust AgCl:Ag hollow nanocrystals. *Applied Catalysis B: Environmental*. 2015;**164**:344-351. DOI: <http://dx.doi.org/10.1016/j.apcatb.2014.09.049>
- [21] Guler U, ShalaeV VM, Boltasseva A. Nanoparticle plasmonics: Going practical with transition metal nitrides. *Materials Today*. 2015;**18**(4):227-237. DOI: <http://dx.doi.org/10.1016/j.mattod.2014.10.039>
- [22] Wang J, Tang L, Zeng G, Liu Y, Zhou Y, Deng Y, et al. Plasmonic Bi metal deposition and g-C<sub>3</sub>N<sub>4</sub> coating on Bi<sub>2</sub>WO<sub>6</sub> microspheres for efficient visible-light photocatalysis. *ACS Sustainable Chemistry and Engineering*. 2017;**5**(1):1062-1072. DOI: 10.1021/acssuschemeng.6b02351
- [23] Huang Y, Kang S, Yang Y, Qin H, Ni Z, Yang S, et al. Facile synthesis of Bi/Bi<sub>2</sub>WO<sub>6</sub> nanocomposite with enhanced photocatalytic activity under visible light. *Applied Catalysis B: Environmental*. 2016;**196**:89-99. DOI: 10.1016/j.apcatb.2016.05.022
- [24] Yu S, Huang H, Dong F, Li M, Tian N, Zhang T, et al. Synchronously achieving plasmonic Bi metal deposition and I<sup>-</sup> doping by utilizing BiOI<sub>3</sub> as the self-sacrificing template for high-performance multifunctional applications. *ACS Applied Materials and Interfaces*. 2015;**7**(50):27925-27933. DOI: 10.1021/acsami.5b09994
- [25] Han J, Zou HY, Liu ZX, Yang T, Gao MX, Huang CZ. Efficient visible-light photocatalytic heterojunctions formed by coupling plasmonic Cu<sub>2-x</sub>Se and graphitic carbon nitride. *New Journal of Chemistry*. 2015;**39**(8):6186-6192. DOI: 10.1039/c5nj01010a

- [26] Meng X, Zhang Z. Pd-doped  $\text{Bi}_2\text{MoO}_6$  plasmonic photocatalysts with enhanced visible light photocatalytic performance. *Applied Surface Science*. 2017;**392**:169-180. DOI: 10.1016/j.apsusc.2016.08.113
- [27] Chen F, Yang Q, Wang Y, Zhao J, Wang D, Li X, et al. Novel ternary heterojunction photocatalyst of Ag nanoparticles and g- $\text{C}_3\text{N}_4$  nanosheets co-modified  $\text{BiVO}_4$  for wider spectrum visible-light photocatalytic degradation of refractory pollutant. *Applied Catalysis B: Environmental*. 2017;**205**:133-147. DOI: <http://dx.doi.org/10.1016/j.apcatb.2016.12.017>
- [28] Wan Y, Liang C, Xia Y, Huang W, Li Z. Fabrication of graphene oxide enwrapped Z-scheme  $\text{Ag}_2\text{SO}_3/\text{AgBr}$  nanoparticles with enhanced visible-light photocatalysis. *Applied Surface Science*. 2017;**396**:48-57. DOI: 10.1016/j.apsusc.2016.10.189
- [29] Ao Y, Bao J, Wang P, Wang C. A novel heterostructured plasmonic photocatalyst with high photocatalytic activity:  $\text{Ag@AgCl}$  nanoparticles modified titanium phosphate nanoplates. *Journal of Alloys and Compounds*. 2017;**698**:451-459. DOI: 10.1016/j.jallcom.2016.12.231
- [30] Liu Y, Zhu G, Gao J, Hojamberdiev M, Zhu R, Wei X, et al. Enhanced photocatalytic activity of  $\text{Bi}_4\text{Ti}_3\text{O}_{12}$  nanosheets by  $\text{Fe}^{3+}$ -doping and the addition of Au nanoparticles: Photodegradation of Phenol and bisphenol A. *Applied Catalysis B: Environmental*. 2017;**200**:72-82. DOI: 10.1016/j.apcatb.2016.06.069
- [31] Levchuk I, Sillanpää M, Guillard C, Gregori D, Chateau D, Chaput F, et al. Enhanced photocatalytic activity through insertion of plasmonic nanostructures into porous  $\text{TiO}_2/\text{SiO}_2$  hybrid composite films. *Journal of Catalysis*. 2016;**342**:117-124. DOI: 10.1016/j.jcat.2016.07.015
- [32] Yan XQ, Zhu XH, Li RH, Chen WX. Au/ $\text{BiOCl}$  heterojunction within mesoporous silica shell as stable plasmonic photocatalyst for efficient organic pollutants decomposition under visible light. *Journal of Hazardous Materials*. 2016;**303**:1-9. DOI: 10.1016/j.jhazmat.2015.10.029
- [33] Chen X, Zhao Q, Li X, Wang D. Enhanced photocatalytic activity of degrading short chain chlorinated paraffins over reduced graphene oxide/ $\text{CoFe}_2\text{O}_4/\text{Ag}$  nanocomposite. *Journal of Colloid and Interface Science*. 2016;**479**:89-97. DOI: 10.1016/j.jcis.2016.06.053
- [34] Song S, Cheng B, Wu N, Meng A, Cao S, Yu J. Structure effect of graphene on the photocatalytic performance of plasmonic  $\text{Ag}/\text{Ag}_2\text{CO}_3\text{-RGO}$  for photocatalytic elimination of pollutants. *Applied Catalysis B: Environmental*. 2016;**181**:71-78. DOI: <http://dx.doi.org/10.1016/j.apcatb.2015.07.034>
- [35] Guo W, Qin Q, Geng L, Wang D, Guo Y, Yang Y. Morphology-controlled preparation and plasmon-enhanced photocatalytic activity of Pt- $\text{BiOBr}$  heterostructures. *Journal of Hazardous Materials*. 2016;**308**:374-385. DOI: <http://dx.doi.org/10.1016/j.jhazmat.2016.01.077>

- [36] Gomez L, Sebastian V, Arruebo M, Santamaria J, Cronin SB. Plasmon-enhanced photocatalytic water purification. *Physical Chemistry Chemical Physics*. 2014;**16**(29):15111-15116. DOI: 10.1039/c4cp00229f
- [37] Friedmann D, Hakki A, Kim H, Choi W, Bahnemann D. Heterogeneous photocatalytic organic synthesis: State-of-the-art and future perspectives. *Green Chemistry*. 2016;**18**(20):5391-5411. DOI: 10.1039/C6GC01582D
- [38] Peiris S, McMurtrie J, Zhu H-Y. Metal nanoparticle photocatalysts: Emerging processes for green organic synthesis. *Catalysis Science & Technology*. 2016;**6**(2):320-338. DOI: 10.1039/C5CY02048D
- [39] Chen J, Cen J, Xu X, Li X. The application of heterogeneous visible light photocatalysts in organic synthesis. *Catalysis Science & Technology*. 2016;**6**(2):349-362. DOI: 10.1039/C5CY01289A
- [40] Lang X, Zhao J, Chen X. Cooperative photoredox catalysis. *Chemical Society Reviews*. 2016;**45**(11):3026-3038. DOI: 10.1039/C5CS00659G
- [41] Cheng H, Fuku K, Kuwahara Y, Mori K, Yamashita H. Harnessing single-active plasmonic nanostructures for enhanced photocatalysis under visible light. *Journal of Materials Chemistry A*. 2015;**3**(10):5244-5258. DOI: 10.1039/c4ta06484d
- [42] Tanaka A, Hashimoto K, Kominami H. Preparation of Au/CeO<sub>2</sub> exhibiting strong surface plasmon resonance effective for selective or chemoselective oxidation of alcohols to aldehydes or ketones in aqueous suspensions under irradiation by green light. *Journal of the American Chemical Society*. 2012;**134**(35):14526-14533. DOI: 10.1021/ja305225s
- [43] Hallett-Tapley GL, Silvero MJ, Bueno-Alejo CJ, Gonzalez-Bejar M, McTiernan CD, Grenier M, et al. Supported gold nanoparticles as efficient catalysts in the solvent less plasmon mediated oxidation of sec-Phenethyl and benzyl alcohol. *Journal of Physical Chemistry C*. 2013;**117**(23):12279-12288. DOI: 10.1021/jp311069v
- [44] Yu J, Li J, Wei H, Zheng J, Su H, Wang X. Hydrotalcite-supported gold catalysts for a selective aerobic oxidation of benzyl alcohol driven by visible light. *Journal of Molecular Catalysis A: Chemical*. 2014;**395**:128-136. DOI: <http://dx.doi.org/10.1016/j.molcata.2014.08.023>
- [45] Chen Y, Li W, Wang J, Yang Q, Hou Q, Ju M. Gold nanoparticle-modified TiO<sub>2</sub>/SBA-15 nanocomposites as active plasmonic photocatalysts for the selective oxidation of aromatic alcohols. *RSC Advances*. 2016;**6**(74):70352-70363. DOI: 10.1039/C6RA11390G
- [46] Pineda A, Gomez L, Balu AM, Sebastian V, Ojeda M, Arruebo M, et al. Laser-driven heterogeneous catalysis: Efficient amide formation catalysed by Au/SiO<sub>2</sub> systems. *Green Chemistry*. 2013;**15**(8):2043-2049. DOI: 10.1039/C3GC40166A
- [47] Xiao Q, Liu Z, Bo A, Zavahir S, Sarina S, Bottle S, et al. Catalytic transformation of aliphatic alcohols to corresponding esters in O<sub>2</sub> under neutral conditions using visible-light irradiation. *Journal of the American Chemical Society*. 2015;**137**(5):1956-1966. DOI: 10.1021/ja511619c



- [48] Zhang Y, Xiao Q, Bao Y, Zhang Y, Bottle S, Sarina S, et al. Direct photocatalytic conversion of aldehydes to esters using supported gold nanoparticles under visible light irradiation at room temperature. *The Journal of Physical Chemistry C*. 2014;**118**(33):19062-19069. DOI: 10.1021/jp505552v
- [49] Alejo CJB, Fasciani C, Grenier M, Netto-Ferreira JC, Scaiano JC. Reduction of resazurin to resorufin catalyzed by gold nanoparticles: Dramatic reaction acceleration by laser or LED plasmon excitation. *Catalysis Science & Technology*. 2011;**1**(8):1506-1511. DOI: 10.1039/C1CY00236H
- [50] Ke X, Zhang X, Zhao J, Sarina S, Barry J, Zhu H. Selective reductions using visible light photocatalysts of supported gold nanoparticles. *Green Chemistry*. 2013;**15**(1):236-244. DOI: 10.1039/C2GC36542A
- [51] Guo X, Hao C, Jin G, Zhu H-Y, Guo X-Y. Copper nanoparticles on graphene support: An efficient photocatalyst for coupling of nitroaromatics in visible light. *Angewandte Chemie International Edition*. 2014;**53**(7):1973-1977. DOI: 10.1002/anie.201309482
- [52] Tokarek K, Hueso JL, Kuśtrowski P, Stochel G, Kyzioł A. Green synthesis of chitosan-stabilized copper nanoparticles. *European Journal of Inorganic Chemistry*. 2013;**2013**(28):4940-4947. DOI: 10.1002/ejic.201300594
- [53] Zhao X, Long R, Liu D, Luo B, Xiong Y. Pd-Ag alloy nanocages: Integration of Ag plasmonic properties with Pd active sites for light-driven catalytic hydrogenation. *Journal of Materials Chemistry A*. 2015;**3**(18):9390-9394. DOI: 10.1039/C5TA00777A
- [54] Wang F, Li C, Chen H, Jiang R, Sun LD, Li Q, et al. Plasmonic harvesting of light energy for Suzuki coupling reactions. *Journal of the American Chemical Society*. 2013;**135**(15):5588-5601. DOI: 10.1021/ja310501y
- [55] Hu YX, Liu YZ, Li Z, Sun YG. Highly asymmetric, interfaced dimers made of Au nanoparticles and bimetallic nanoshells: Synthesis and photo-enhanced catalysis. *Advanced Functional Materials*. 2014;**24**(19):2828-2836. DOI: 10.1002/adfm.201303557
- [56] Cui J, Li Y, Liu L, Chen L, Xu J, Ma J, et al. Near-infrared plasmonic-enhanced solar energy harvest for highly efficient photocatalytic reactions. *Nano Letters*. 2015;**15**(10):6295-6301. DOI: 10.1021/acs.nanolett.5b00950
- [57] Lou Z, Gu Q, Liao Y, Yu S, Xue C. Promoting Pd-catalyzed Suzuki coupling reactions through near-infrared plasmon excitation of WO<sub>3-x</sub> nanowires. *Applied Catalysis B: Environmental*. 2016;**184**:258-263. DOI: 10.1016/j.apcatb.2015.11.037
- [58] Cheng H, Kamegawa T, Mori K, Yamashita H. Surfactant-free nonaqueous synthesis of plasmonic molybdenum oxide nanosheets with enhanced catalytic activity for hydrogen generation from ammonia borane under visible light. *Angewandte Chemie International Edition*. 2014;**53**(11):2910-2914. DOI: 10.1002/anie.201309759
- [59] Li Q, Mahendra S, Lyon DY, Brunet L, Liga MV, Li D, et al. Antimicrobial nanomaterials for water disinfection and microbial control: Potential applications and implications. *Water Research*. 2008;**42**(18):4591-4602. DOI: <http://dx.doi.org/10.1016/j.watres.2008.08.015>

- [60] Tian B, Dong R, Zhang J, Bao S, Yang F, Zhang J. Sandwich-structured AgCl at Ag at TiO<sub>2</sub> with excellent visible-light photocatalytic activity for organic pollutant degradation and *E. coli* K12 inactivation. *Applied Catalysis B: Environmental*. 2014;**158-159**:76-84. DOI: 10.1016/j.apcatb.2014.04.008
- [61] Shi H, Li G, Sun H, An T, Zhao H, Wong P-K. Visible-light-driven photocatalytic inactivation of *E. coli* by Ag/AgX-CNTs (X = Cl, Br, I) plasmonic photocatalysts: Bacterial performance and deactivation mechanism. *Applied Catalysis B: Environmental*. 2014;**158-159**:301-307. DOI: <http://dx.doi.org/10.1016/j.apcatb.2014.04.033>
- [62] Xia D, An T, Li G, Wang W, Zhao H, Wong PK. Synergistic photocatalytic inactivation mechanisms of bacteria by graphene sheets grafted plasmonic AgAgX (X = Cl, Br, I) composite photocatalyst under visible light irradiation. *Water Research*. 2016;**99**:149-161. DOI: 10.1016/j.watres.2016.04.055
- [63] Sarkar AK, Saha A, Tarafder A, Panda AB, Pal S. Efficient removal of toxic dyes via simultaneous adsorption and solar light driven photodegradation using recyclable functionalized Amylopectin-TiO<sub>2</sub>-Au nanocomposite. *ACS Sustainable Chemistry and Engineering*. 2016;**4**(3):1679-1688. DOI: 10.1021/acssuschemeng.5b01614
- [64] Li C, Yang W, Liu L, Sun W, Li Q. In situ growth of TiO<sub>2</sub> on TiN nanoparticles for non-noble-metal plasmonic photocatalysis. *RSC Advances*. 2016;**6**(76):72659-72669. DOI: 10.1039/c6ra15435b
- [65] Ren H, Koshy P, Chen W-F, Qi S, Sorrell CC. Photocatalytic materials and technologies for air purification. *Journal of Hazardous Materials*. 2017;**325**:340-366. DOI: <http://dx.doi.org/10.1016/j.jhazmat.2016.08.072>
- [66] Chen X, Zhu H-Y, Zhao J-C, Zheng Z-F, Gao X-P. Visible-light-driven oxidation of organic contaminants in air with gold nanoparticle catalysts on oxide supports. *Angewandte Chemie*. 2008;**120**(29):5433-5436. DOI: 10.1002/ange.200800602
- [67] Dinh C-T, Yen H, Kleitz F, Do T-O. Three-dimensional ordered assembly of thin-shell Au/TiO<sub>2</sub> hollow nanospheres for enhanced visible-light-driven photocatalysis. *Angewandte Chemie International Edition*. 2014;**53**(26):6618-6623. DOI: 10.1002/anie.201400966
- [68] Sellappan R, Nielsen MG, González-Posada F, Vesborg PCK, Chorkendorff I, Chakarova D. Effects of plasmon excitation on photocatalytic activity of Ag/TiO<sub>2</sub> and Au/TiO<sub>2</sub> nanocomposites. *Journal of Catalysis*. 2013;**307**:214-221. DOI: <http://dx.doi.org/10.1016/j.jcat.2013.07.024>
- [69] Inoue T, Fujishima A, Konishi S, Honda K. Photoelectrocatalytic reduction of carbon dioxide in aqueous suspensions of semiconductor powders. *Nature*. 1979;**277**(5698):637-638
- [70] Liu HM, Meng XG, Dao TD, Zhang HB, Li P, Chang K, et al. Conversion of carbon dioxide by methane reforming under visible-light irradiation: Surface-plasmon-mediated nonpolar molecule activation. *Angewandte Chemie-International Edition*. 2015;**54**(39):11545-11549. DOI: 10.1002/anie.201504933

- [71] Upadhye AA, Ro I, Zeng X, Kim HJ, Tejedor I, Anderson MA, et al. Plasmon-enhanced reverse water gas shift reaction over oxide supported Au catalysts. *Catalysis Science & Technology*. 2015;**5**(5):2590-2601. DOI: 10.1039/C4CY01183J
- [72] Shown I, Hsu H-C, Chang Y-C, Lin C-H, Roy PK, Ganguly A, et al. Highly efficient visible light photocatalytic reduction of CO<sub>2</sub> to hydrocarbon fuels by Cu-nanoparticle decorated graphene oxide. *Nano Letters*. 2014;**14**(11):6097-6103. DOI: 10.1021/nl503609v
- [73] Yuliaty L, Itoh H, Yoshida H. Photocatalytic conversion of methane and carbon dioxide over gallium oxide. *Chemical Physics Letters*. 2008;**452**(1--3):178-182. DOI: <http://dx.doi.org/10.1016/j.cplett.2007.12.051>
- [74] Baldoví HG, Neaţu Ş, Khan A, Asiri AM, Kosa SA, Garcia H. Understanding the origin of the photocatalytic CO<sub>2</sub> reduction by Au- and Cu-loaded TiO<sub>2</sub>: A microsecond transient absorption spectroscopy study. *The Journal of Physical Chemistry C*. 2015;**119**(12):6819-6827. DOI: 10.1021/jp5106136
- [75] Tahir B, Tahir M, Amin NS. Gold-indium modified TiO<sub>2</sub> nanocatalysts for photocatalytic CO<sub>2</sub> reduction with H<sub>2</sub> as reductant in a monolith photoreactor. *Applied Surface Science*. 2015;**338**:1-14. DOI: <http://dx.doi.org/10.1016/j.apsusc.2015.02.126>
- [76] Tan L-L, Ong W-J, Chai S-P, Mohamed AR. Noble metal modified reduced graphene oxide/TiO<sub>2</sub> ternary nanostructures for efficient visible-light-driven photoreduction of carbon dioxide into methane. *Applied Catalysis B: Environmental*. 2015;**166-167**:251-259. DOI: <http://dx.doi.org/10.1016/j.apcatb.2014.11.035>
- [77] Vaiano V, Sannino D, Ciambelli P. Steam reduction of CO<sub>2</sub> on Pd/TiO<sub>2</sub> catalysts: A comparison between thermal and photocatalytic reactions. *Photochemical & Photobiological Sciences*. 2015;**14**(3):550-555. DOI: 10.1039/C4PP00252K
- [78] Yang K, Liu J, Si R, Chen X, Dai W, Fu X. Comparative study of Au/TiO<sub>2</sub> and Au/Al<sub>2</sub>O<sub>3</sub> for oxidizing CO in the presence of H<sub>2</sub> under visible light irradiation. *Journal of Catalysis*. 2014;**317**:229-239. DOI: <http://dx.doi.org/10.1016/j.jcat.2014.06.005>
- [79] Yui T, Kan A, Saitoh C, Koike K, Ibusuki T, Ishitani O. Photochemical reduction of CO<sub>2</sub> using TiO<sub>2</sub>: Effects of organic adsorbates on TiO<sub>2</sub> and deposition of Pd onto TiO<sub>2</sub>. *ACS Applied Materials & Interfaces*. 2011;**3**(7):2594-2600. DOI: 10.1021/am200425y
- [80] Zhai Q, Xie S, Fan W, Zhang Q, Wang Y, Deng W, et al. Photocatalytic conversion of carbon dioxide with water into methane: Platinum and copper(I) oxide Co-catalysts with a Core-Shell structure. *Angewandte Chemie International Edition*. 2013;**52**(22):5776-5779. DOI: 10.1002/anie.201301473
- [81] Zhang X, Li X, Zhang D, Su NQ, Yang W, Everitt HO, et al. Product selectivity in plasmonic photocatalysis for carbon dioxide hydrogenation. *Nature Communications*. 2017;**8**:14542. DOI: 10.1038/ncomms14542 <http://www.nature.com/articles/ncomms14542#supplementary-information>

- [82] Putri LK, Ong W-J, Chang WS, Chai S-P. Enhancement in the photocatalytic activity of carbon nitride through hybridization with light-sensitive AgCl for carbon dioxide reduction to methane. *Catalysis Science & Technology*. 2016;**6**(3):744-754. DOI: 10.1039/C5CY00767D
- [83] Macia-Agullo JA, Corma A, Garcia H. Photobiocatalysis: The power of combining photocatalysis and enzymes. *Chemistry-a European Journal*. 2015;**21**(31):10940-10959. DOI: 10.1002/chem.201406437
- [84] Sanchez-Iglesias A, Barroso J, Solis DM, Taboada JM, Obelleiro F, Pavlov V, et al. Plasmonic substrates comprising gold nanostars efficiently regenerate cofactor molecules. *Journal of Materials Chemistry A*. 2016;**4**(18):7045-7052. DOI: 10.1039/c6ta01770c
- [85] Sanchez-Iglesias A, Chuvilin A, Grzelczak M. Plasmon-driven photoregeneration of cofactor molecules. *Chemical Communications*. 2015;**51**(25):5330-5333. DOI: 10.1039/c4cc07829b
- [86] Lin YH, Ren JS, Qu XG. Catalytically active nanomaterials: A promising candidate for artificial enzymes. *Accounts of Chemical Research*. 2014;**47**(4):1097-1105. DOI: 10.1021/ar400250z
- [87] Ortega-Liebana MC, Hueso JL, Arenal R, Santamaria J. Titania-coated gold nanorods with expanded photocatalytic response. Enzyme-like glucose oxidation under near-infrared illumination. *Nanoscale*. 2017;**9**(5):1787-1792. DOI: 10.1039/C6NR06300D
- [88] Zhou BW, Song JL, Zhou HC, Wu TB, Han BX. Using the hydrogen and oxygen in water directly for hydrogenation reactions and glucose oxidation by photocatalysis. *Chemical Science*. 2016;**7**(1):463-468. DOI: 10.1039/c5sc03178h
- [89] Primo A, Corma A, Garcia H. Titania supported gold nanoparticles as photocatalyst. *Physical Chemistry Chemical Physics*. 2011;**13**(3):886-910. DOI: 10.1039/c0cp00917b